ISSN: 2573-9514

Research Article

Journal of Addiction Research

The Anger Feedback Loop Cascade (ALC) as a Distinct Developmental Risk Pathway to Extreme Behavioral and Sudden Death

Travis Hawkins*

Independent Research, Co, Concept Association, Inc, USA

***Corresponding Author**
Travis Hawkins, Independent Research, Co, Concept Association, Inc, USA.

Submitted: 2026, Mar 18; **Accepted:** 2026, Apr 15; **Published:** 2026, Apr 30

Citation: Hawkins, T. (2026). The Anger Feedback Loop Cascade (ALC) as a Distinct Developmental Risk Pathway to Extreme Behavioral and Sudden Death. *J Addict Res, 10*(1), 01-32.

Abstract

This study advances a recursive systems model of harm enactment that quantifies both the window of highest harm probability and the trajectory of severity escalation. Extending Worldview Coherence is Not Optional (DOI: 10.33140/JAR.10.01.02), we analyze a large-scale meta-analytic dataset ($k > 1{,}000$ outcomes; $N > 29{,}000{,}000$ participants). Threshold 1 identifies the instability boundary at which bilateral amplification of Epistemic Disorientation (EpD) and Affective Dysregulation (AD) are embodied by Physiological Load (PL) and produce a recursive escalation dominant eigenvalue (λ_1) exceeding restraints, initiating a self-excitatory recursive anger feedback loop cascade (ALC). Monte Carlo calibration indicates overt harm becomes highly probable within approximately 29 days in dampened (treated) samples following instability onset. Threshold 2 models recursive severity gain. On a severity scale of 1 to 4, 1 being sub-detection harm and 4 being fatal or lethal harm, initial onset harm severity was estimated at $E(S)_0 = 1.62$, with a nonlinear gain of ~1.7X per cycle. Under undampened conditions, projections indicate migration toward terminal severity within approximately 3.5 years. Recurrence intervals averaged ~1.28 years in treated cohorts. These findings provide a falsifiable, probabilistically defined framework for predicting both harm onset and escalation.

1. Introduction

1.1. Preface: Addendum to *Worldview Coherence is Not Optional*

To mitigate the possibility that prior findings were dependent on repeated analysis of a single dataset, a new and independent dataset was harvested, relevant effects were extracted, and the previously specified modeling framework was reapplied. This addendum therefore functions as a replication and extension, testing the robustness of the original model under novel empirical conditions. From the outset of this research program, a guiding methodological philosophy was adopted: extreme conditions of human experience and behavior are maximally informative about the structure of the system in which they occur. In the search for order and symmetry, extreme states were theorized to reveal most clearly the organizing principles that fail when coherence breaks down. In effect, order is often most visible at its points of rupture.

Accordingly, prior analyses of worldview included both severe disruptions such as post-traumatic stress disorder and moral injury and highly coherent cases, including daily practitioners of both theistic and non-theistic belief systems. The dataset on which the present manuscript rests follows this same logic.

Early analysis of the new dataset yielded several central observations consistent with, and strengthening, prior empirical results.

(a) First, two universal imperatives were supported across datasets: humanity, writ large, exhibits a developmental vulnerability toward narcissism that requires regulation rather than eradication; and the structure and organization of paradigmatic principles—that is, worldview coherence is a psychic and epistemic necessity independent of worldview content [1-3].

(b) Second, the order of virtue acquisition functions as a non-negotiable instruction set for durable well-being and for the emergence of unilateral forgiveness, with deviations from this order reliably associated with destabilization.

(c) Third, a previously unarticulated regime ("Person 4") was empirically indicated, characterized by power-based stabilization rather than loss of control.

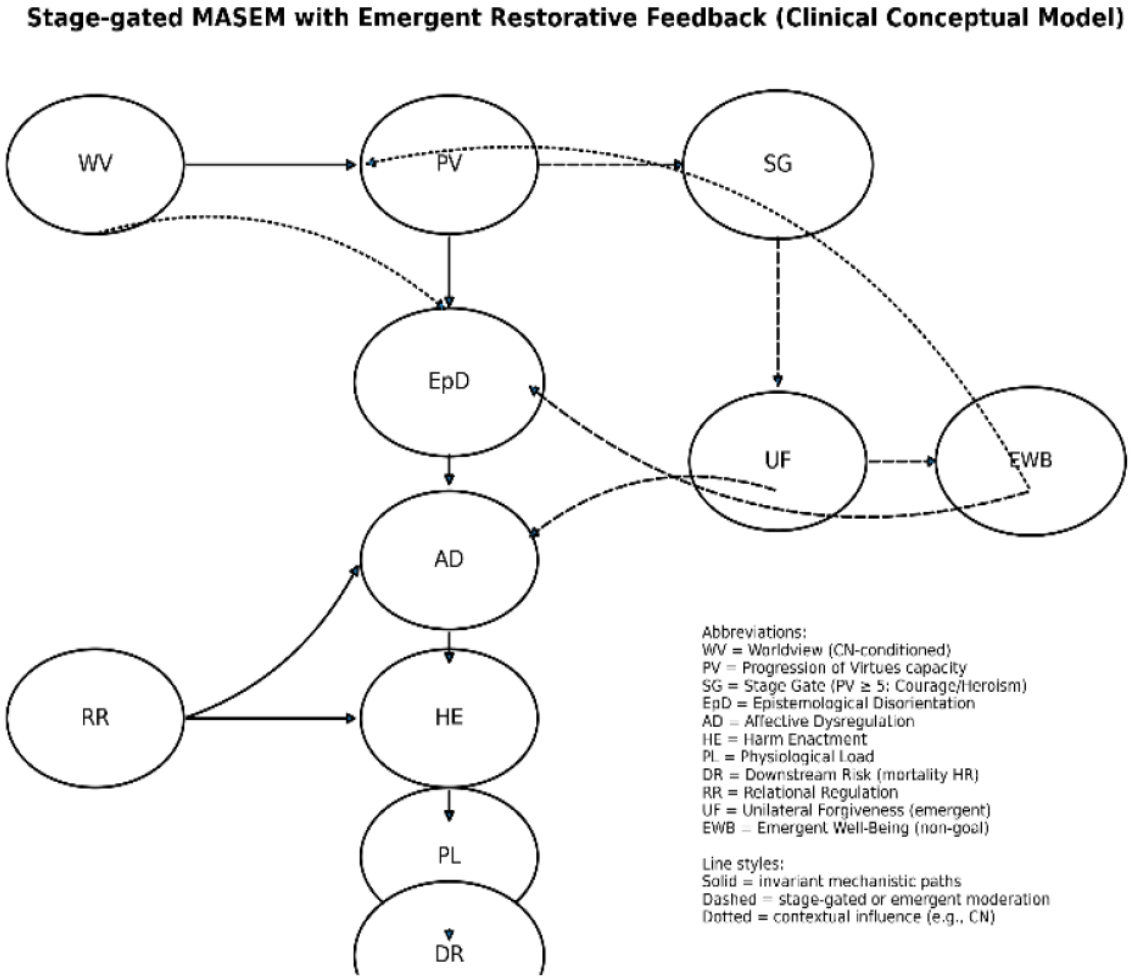

Figure 1: The Holistic Model Identified in "Worldview Coherence is Not Optional"

The directional interpretation of variable interaction is for illustration only. Also identified by ibid., the subsystem Anger Feedback Loop Cascade in Figure 2.

Figure 2: The Anger Feedback Loop Cascade (ALC) is modeled as an emergent amplification subsystem arising from reciprocal coupling among EpD, AD, RR, and PL. It is not treated as a directly observed variable but as a dynamic gain structure. Harm enactment occurs when escalating system pressure exceeds discharge thresholds under conditions of insufficient resistance or damping. The ALC is a direct subsystem of the holistic model and assumes system control once activated.

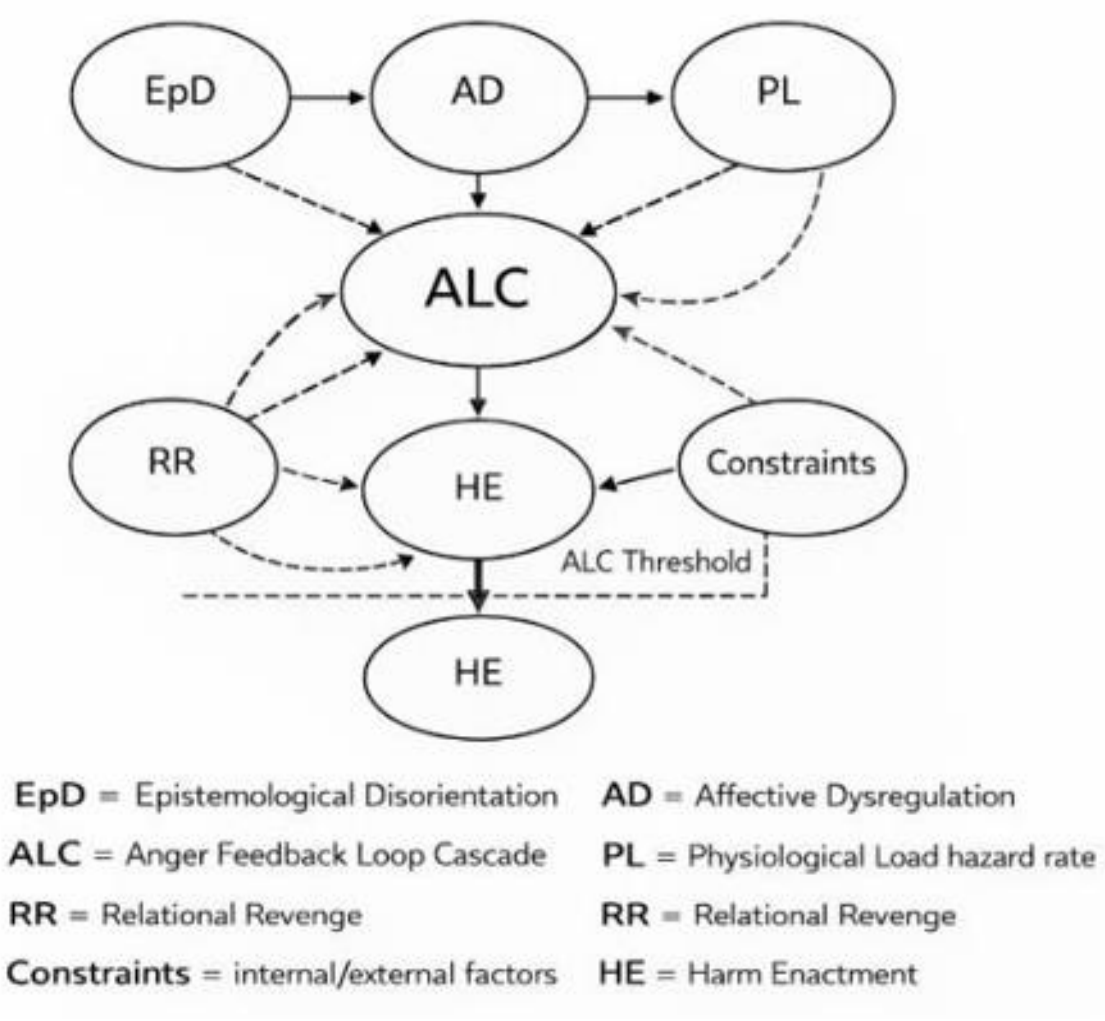

Figure 2: The Anger Feedback Loop Cascade: A Controlling Subsystem

Instead, It Identifies an Externally Regulated Baseline State (Person 0) As the Dominant Control Condition Under Typical Circumstances, In Which Behavior Is Regulated Primarily Through Cultural Narcissism, Impression Management, And Reputation Sensitivity. Prosocial Behavior in This Regime Is Contingent on Observation Rather Than Internally Regulated Coherence. From This Baseline, Divergent Pathways Emerge Under Stress and Destabilization (Person 1), Under Power-Based Substitution and Grievance (Person 4), Or Through Developmental Transformation Toward Internally Regulated Coherence (Person 2) And, In Rare Cases, Full Functional Integration (Person 3).

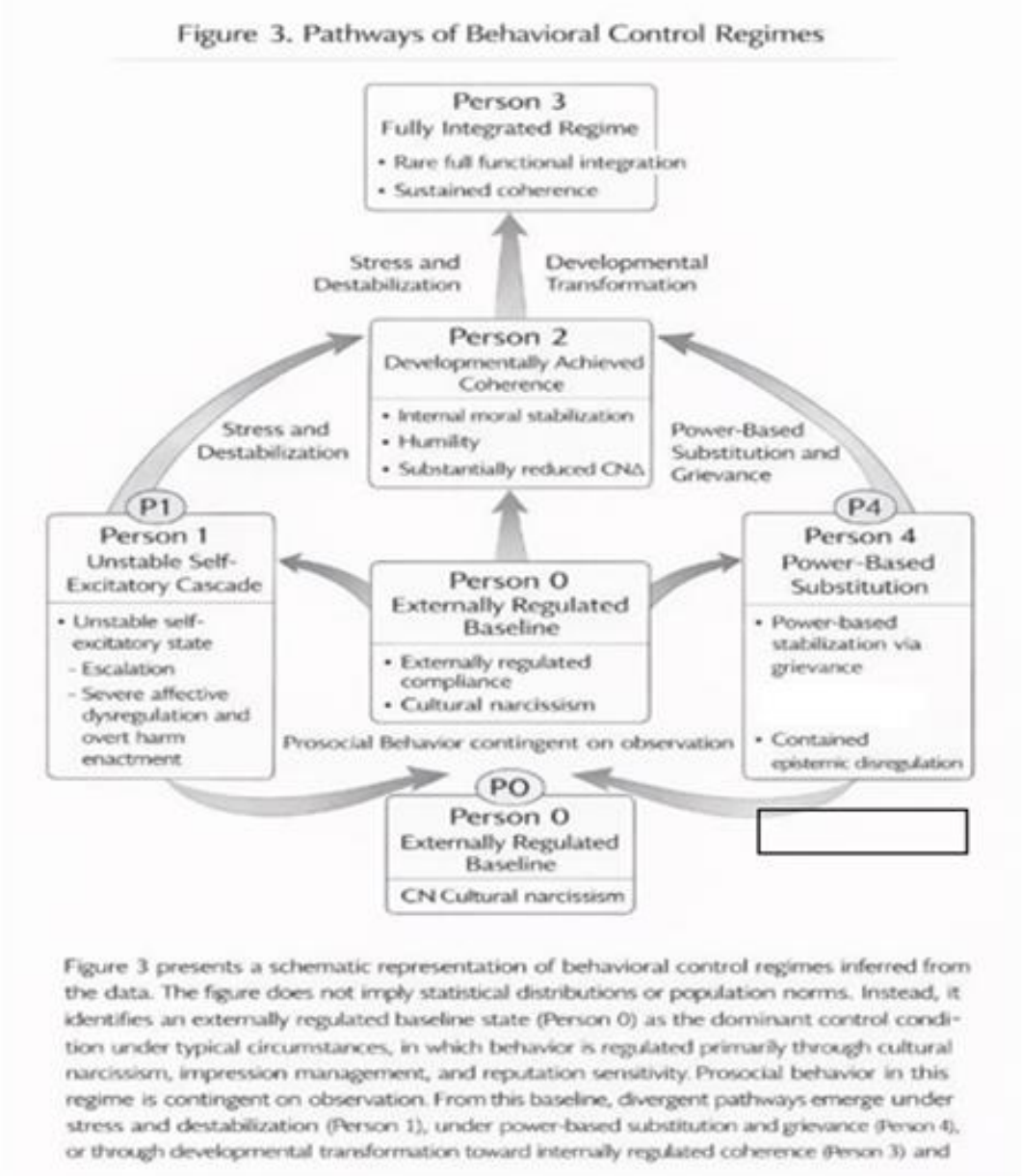

Figure 3: Presents A Schematic Representation of Behavioral Control Regimes Inferred from the Data. The Figure Does Not Imply Statistical Distributions or Population Norms

The present findings both validate and extend the empirically identified model. The newly identified regime, Person 4, is mechanistically congruent with all prior constructs. Figures 4a and 4b illustrate the bifurcation of Person 4 from Person 1 following activation of the Anger Loop Cascade (ALC), at which point the ALC becomes the dominant subsystem governing overall system stability.

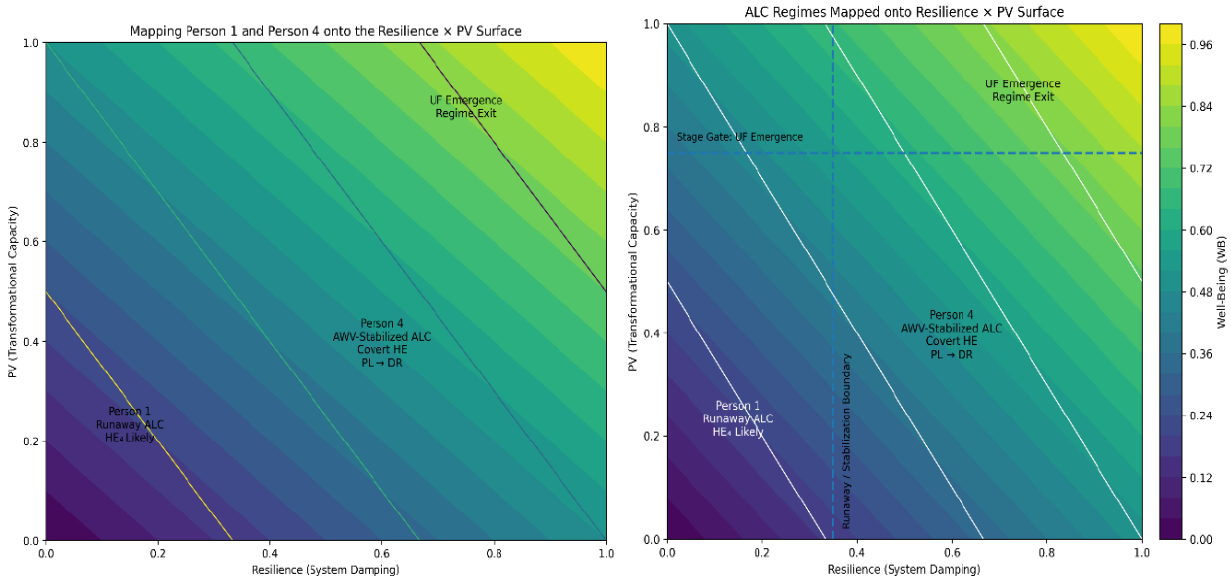

Figures 4a and 4b: Illustrate the Bifurcation Process Between Person 1(Pathological) and Person 4 (Chronic Sub-Detection HE). Resilience Here is Defined as a Static System Condition of Adaptive Ability Either Innate or Learned [4]

In Person 1, low resilience (resilience is here defined as an inherent capacity for adaptation, inherited or experiential) permits the ALC to spiral out of control, producing exponential gain escalation and a high probability of detectable pathological harm enactment. In contrast, in Person 4, average to high resilience treated here as a static system condition proves detrimental. Rather than destabilizing the system, resilience enables a reorientation of control around relational revenge (RR) and grievance. This reorientation partially attenuates ALC gain and produces a form of control-stability rather than health. Worldview coherence in Person 4 is virtually absent, while cultural narcissism is amplified through power and entitlement. Crucially, epistemic disorientation (EpD) does not resolve but becomes phenotypically suppressed: legitimate worldview coherence is substituted by anger, revenge, and grievance as the organizing principles of behavior. Affective dysregulation (AD) is reduced to a tolerable range, allowing the system to reach a state of apparent stability.

Within this regime, Person 4 predominantly engages in socially acceptable harm enactment or, at worst, chronic abusive behaviors that fall below reporting thresholds, including psychological and emotional abuse, intimidation, control, dominance, threats, and aggression short of overt violence. On rare occasions, Person 4 may exceed the harm-enactment threshold and trigger mandatory intervention, but such events are infrequently reported. More commonly, Person 4 is socially rewarded for narcissistic impression and reputation management, elevated standards, ambition, and performative success, and may therefore achieve high levels of external accomplishment.

Importantly, once the ALC is activated, physiological load (PL) and mortality risk (MR) increase across regimes, irrespective of whether the individual follows a Person 1 or Person 4 pathway. PL and ALC operate in a bidirectional relationship, with physiological strain both resulting from and amplifying ALC dynamics. The distinction between regimes thus lies not in health risk which is shared but in the mode of behavioral expression, control strategy, and detectability. This framework allows for explicit investigation of the degree to which destabilization is driven by cognitive–epistemic factors versus physiological coupling. While Person 4 is treated here as an integrated component of the broader model, its characteristics, dynamics, and implications warrant dedicated examination. The present findings therefore establish Person 4 not as a categorical anomaly, but as a coherent and empirically grounded regime—one that merits full treatment in its own right. Resilience, as here defined, represents the static system condition catalyzing the bifurcation of Person1 and Person 4 at the instantiation of the anger feedback loop cascade. It does not provide any dampening or constraining factor in ALC initiation or escalation nor the transition from ALC self-excitation and gain to behavioral harm enactment. As such, resilience is outside the scope of this study.

1.2. Sidebar A: Detection-Layer Inhibition and Physiological Load in ALC Activation

1.2.1. Inhibitory Conditions and Behavioral Detectability

Preliminary analyses identified two adjacent but analytically distinct inhibitory conditions that appear to restrain behavioral detection of an active Anger Feedback Loop Cascade (ALC). First, the structural configuration underlying observable ALC activation (Regime 1/ Person 1) is characterized by high cultural narcissism (CN) and low worldview (WV) coherence. Within this regime, the combination of elevated CN and high socioeconomic status (SES) appears to increase inhibitory pressure on overt behavioral expression. CN confers strong motivational incentives for impression management, reputational preservation, and social

positioning. When coupled with high SES where reputational, occupational, and legal consequences are amplified—this configuration may suppress overt manifestations of relational revenge (RR) and harm enactment (HE), even when internal instability remains active. Second, exogenous restraint mechanisms emerged as a distinct inhibitory pathway. Institutional supervision, legal constraints, psychological hospitalization, incarceration, and parole function as follows.

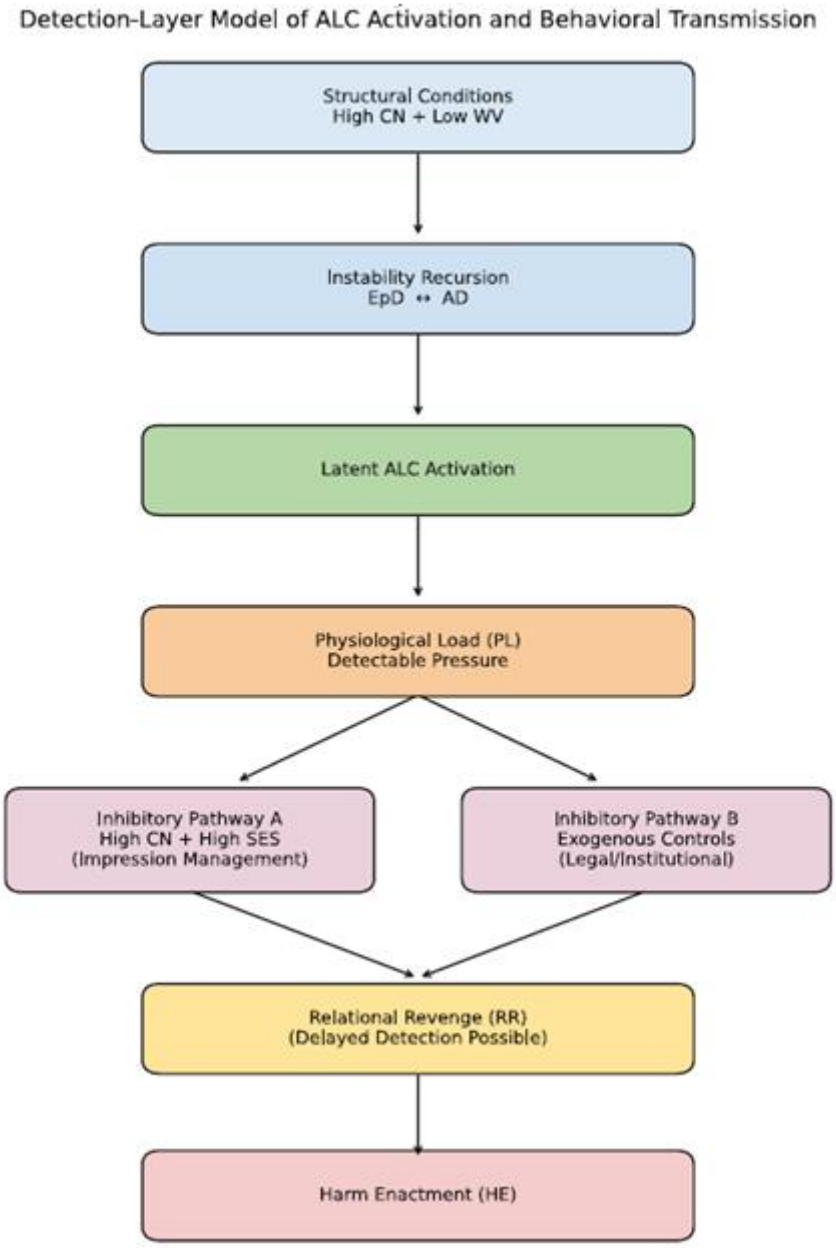

Figure 5: Presents the Transmission Pathway of Detectable Markers within the ALC

1.2.2. Physiological Load as a Concurrent Marker of Instability

Physiological load (PL) emerged as the most consistent concurrent indicator of instability within Epistemic Disorientation (EpD) and Affective Dysregulation (AD) contexts. In the current dataset, approximately 80% of PL-coded rows co-occurred with EpD and/or AD constructs, indicating strong structural convergence between physiological burden and core instability components. PL frequently appeared in the absence of RR coding, demonstrating that detectable physiological strain does not require concurrent behavioral discharge. The data indicate a strong relation between the EpD and AD escalation corridor and physiological load (PL). Although longitudinal evidence was sparse, the coefficient magnitudes within a self-excitatory recursive multilateral dynamic regime showed a significant preference for PL occurring prior to RR. EpD and AD in the escalation corridor are strong attractors for PL binding and model fit statistics suggested the proper order was indeed EpD AD PL RR HE. See Threshold 1 and 2 sections for detailed analytical findings.

1.2.3. Data Definitions and Dataset Structure

The present study draws on two analytically distinct but complementary data resources.

• The first, DATA v40u, is the primary outcome-linked master dataset. It contains coded rows from observational, registry, cohort, case-control, and meta-analytic studies relevant to the ALC framework, with each row mapped into one or more latent construct domains. This sheet is used to estimate downstream and threshold-relevant relations involving EpD, AD, RR, HE, PL, and DR, while also retaining upstream WV and CN coding where available.

• The second, WV CN Guided, is a guided edge bank designed to clarify the upstream structure connecting worldview coherence (WV), cultural narcissism (CN), and the loading of epistemic disorientation (EpD) and affective dysregulation (AD). It is not a mortality-outcome sheet in the same sense as V40u. Rather, it functions as a construct-relations sheet, preserving pairwise edges and theoretical recoding rules needed to define upstream susceptibility and corridor entry.

Together, these resources support the full staged model shown in the stage-gated MASEM figure: WV and CN operate upstream; EpD and AD form the destabilization corridor; RR and HE express relational and behavioral transmission; PL accumulates as concurrent physiological amplification and downstream burden; DR represents terminal mortality-linked risk. The broader clinical conceptual model also includes PV, SG, UF, and EWB as stage-gating and restorative feedback constructs, though these are not equally represented as direct coded rows in the current two main sheets. All extracted data, coding decisions, and construct mappings are intended for public release through OSF under the project title *The Progression of Virtues: A Meta- Analysis*.

1.2.4. Construct Definitions and Placement in the Model

(i) WV: Worldview Coherence

• **Code:** WV

• **Definition:** The degree of meaning, coherence, integration, future orientation, and stable interpretive structure available to the person [5,6]. In the model, WV is protective and occupies the upper-left upstream position. Low WV creates an epistemic vacuum and increases susceptibility to EpD loading.

• **Model location:** Upstream protective input feeding PV and moderating EpD vulnerability.

(ii) CN: Cultural Narcissism

• **Code:** CN

• **Definition:** Entitlement, antagonism, grievance-based self-reference, externalized blame, and narcissistic amplification. CN functions as a destabilizing contextual pressure that interacts with low WV to load EpD.

• **Model location:** Upstream destabilizing amplifier conditioning WV and contributing to EpD preloading.

(iii) EpD: Epistemic Disorientation

• **Code:** EpD

• **Definition:** Distress, hopelessness, confusion, identity diffusion, fragmentation, collapse of meaning, and epistemic incoherence. EpD is the first major destabilization reservoir in the ALC model.

• **Model location:** Primary internal instability node downstream of WV/CN and upstream of AD.

(iv) AD: Affective Dysregulation

• **Code:** AD

• **Definition:** Emotional volatility, impulsive affective reactivity, anger instability, dysregulated distress, and acute loss of emotional control. In the model, AD is recruited by rising EpD and then enters recursive exchange with it.

• **Model location:** Core corridor node downstream of EpD and upstream of HE; forms the EpD– AD escalation corridor.

(v) RR: Relational Revenge Orientation

• **Code:** RR

• **Definition:** Rumination, grievance fixation, revenge orientation, harm fantasy, and hostile interpersonal preoccupation [7,8]. RR is not the beginning of the cascade, but a later expression that helps transmit internal instability into relational or behavioral channels.

• **Model location:** Interpersonal transmission node linking internal instability to harm enactment pathways.

(vi) HE: Harm Enactment

• **Code:** HE

• **Definition:** Self- or other-directed harmful action, including suicide, overdose, accidental preventable death, homicide, IPV lethality, self-destructive behavior, abuse, and related terminal or near-terminal discharge events.

• **Model location:** Behavioral discharge node; the pressure-release valve of the active cascade.

(vii) PL: Physiological Load

• **Code:** PL

• **Definition:** Chronic physiological burden, allostatic load, inflammatory and stress-biomarker proxies, long-term morbidity, and physiologic cost accumulation. In the model, PL is not the origin of Threshold 1 but is the most consistent concurrent recruitment marker of active cascade instability in the current measurement framework.

• **Model location:** Concurrent amplifier and downstream accumulation node beneath HE and alongside active cascade recruitment.

(viii) DR: Downstream Mortality Risk

• **Code:** DR

• **Definition:** A mortality-linked summary risk construct capturing elevated hazard associated with chronic disease burden, behavioral instability, and terminal event susceptibility.

• **Model location:** Furthest downstream mortality endpoint node.

(ix) PV: Progression of Virtues

• **Code:** PV

• **Definition:** Transformational capacity indexed through the staged virtue framework. PV is not heavily represented as a direct coded construct in the current outcome dataset but is central to the

conceptual model as the capacity that gates restorative feedback and stage progression.
• **Model location:** Upstream stage-gating and resilience structure between WV and SG.

(x) SG: Stage Gate
• **Code:** conceptual; not directly coded as a dominant row-wise construct in the two main sheets
• **Definition:** The threshold at which PV reaches sufficient maturity to permit Courage/Heroism level buffering and restorative recursion.
• **Model location:** Gate between PV and emergent restorative pathways.

(xi) UF: Unilateral Forgiveness
• **Code:** conceptual/sparse proxy representation
• **Definition:** An emergent restorative regulatory process that can dampen EpD–AD escalation and support transition toward non-reactive integration.
• **Model location:** Restorative feedback node between SG and EWB, with feedback toward EpD/AD regulation.

(xii) EWB: Emergent Well-Being
• **Code:** conceptual
• **Definition:** A non-goal restorative state emerging under sufficiently developed PV and SG conditions. It is not the target of Threshold 1 analysis but remains part of the broader stage-gated model.
• **Model location:** Distal restorative endpoint.

(xiii) EC: Exogenous Controls
• **Code:** EC
• **Definition:** A damping factor in the overt discharge of HE. Fear of legal and or social consequences brought about by detectable HE.
• **Model location:** Threshold 2 between RR and overt HE.

1.2.5. Verified Construct Coverage: V40u (DATA Tab)
These are non-exclusive row counts based on whether each code appears in Construct Codes. Because rows can carry multiple construct codes, counts do not sum to the total row count.

Construct	k (rows)	Total N	Mean N	Median N	Min N	Max N
WV	73	6,714,066	167,851.65	40,346.0	6	3,663,205
CN	62	3,050,861	78,227.21	40,346.0	6	333,009
EpD	213	21,286,211	191,767.67	103.0	1	13,382,552
AD	231	21,431,724	186,362.82	276.0	1	13,382,552
RR	157	57,040	1,296.36	222.0	1	20,550
HE	291	28,895,092	222,269.94	572.0	1	13,382,552
PL	152	74,157	583.91	213.0	36	7,682
DR	30	518,968	37,069.14	13,524.0	884	139,252

Table 1: "Data v40u" Spreadsheet in "v40u_Master_Dataset" Workbook per Construct Descriptive Statistics

• **Interpretation**
V40u is heavily populated in EpD, AD, and HE, with substantial coverage for WV and CN and meaningful but smaller dedicated coverage for RR, PL, and DR. This is exactly what would be expected from a threshold-oriented behavioral and mortality dataset: extensive acute-outcome coverage, strong internal-instability coverage, and more selective but still usable physiological and mortality-risk coverage.

1.2.6. Verified Construct Coverage: WV CN Guided
These are edge-level mapped counts, not row-wise construct-code counts. I applied your canonical interpretive rules to the edge sheet so that constructs such as PTSD, moral injury, affective dysregulation, spirituality, purpose, DSES, ANON, MASK+, INFORM+, INFORM−, and related indicators are mapped into the model's upstream constructs. These counts are therefore best understood as the number of usable guided edges involving each construct, with _ total summed where reported.

Construct	k (edges)	Total N (reported)	Mean N	Median N	Min N	Max N
WV	227	172,638	2,926.07	2,118.0	77	5,449
CN	64	1,722	191.33	150.0	150	336
EpD	141	50,110	365.77	161.0	23	1,754
AD	141	50,110	365.77	161.0	23	1,754
RR	0	0	—	—	—	—
HE	0	0	—	—	—	—
PL	0	0	—	—	—	—
DR	0	0	—	—	—	—

Table 2: "WV CN Guided" Spreadsheet in "v40u_Master_Dataset" Workbook per Construct Descriptive Statistics

• Interpretation

This is exactly the sheet's intended role: WV CN Guided is an upstream and corridor definition sheet, not a downstream mortality sheet. It is rich in WV, CN, and EpD/AD corridor proxies, but it does not serve as the primary source for RR, HE, PL, or DR estimation. Those constructs belong mainly to V40u.

1.2.7. Basic Dataset Statistics

Statistic	Value
Total rows (k)	580
Total cumulative N	29,074,677
Mean sample size	107,683.99
Median sample size	268.5
Minimum N	1
Maximum N	13,382,552

Table 3: v40u Spreadsheet Overall Descriptive Statistics

Statistic	Value
Total rows (k)	711
Total reported N	258,146
Mean reported N	872.11
Median reported N	161.0
Minimum N	23
Maximum N	6,423
Rows with reported N present	296

Table 4: WV CN Guided Spreadsheet Overall Descriptive Statistics

The analytic dataset was organized into two complementary components. The V40u master sheet served as the primary outcome-linked dataset and contained 580 coded rows with a cumulative reported sample size of 29,074,677 participants. It provided the main empirical basis for modeling EpD, AD, RR, HE, PL, and DR in relation to behavioral and mortality-linked outcomes. The WV CN Guided sheet served a different but equally important role: it contained 711 guided construct edges used to define the upstream susceptibility structure linking worldview coherence and cultural narcissism to epistemic disorientation and entry into the EpD– AD corridor. Together, these resources provided both the upstream conceptual architecture and the downstream observational anchor needed for threshold modeling. All coded datasets, extraction files, and construct mappings are being made publicly available through OSF under the project title *The Progression of Virtues: A Meta-Analysis*. One important transparency sentence should probably be added: The V40u counts are row-wise construct-code counts and are therefore non-exclusive; the WV CN Guided counts are edge-level mapped counts and are likewise non-exclusive under the prespecified interpretive recoding rules.

1.3. Data Collection and Coding Procedures

1.3.1. Study Identification and Screening

A systematic literature search was conducted to identify published cohort, registry-based, case– control, and meta-analytic studies reporting associations between behavioral,

psychological, physiological, and environmental exposures and extreme harm-related or mortality outcomes. Searches were performed across major bibliographic and registry databases (e.g., PubMed, PsycINFO, Scopus, Web of Science, national mortality registries, and addiction and violence surveillance systems) using combinations of keywords related to suicidality, substance use, interpersonal violence, accidental death, emotional dysregulation, social isolation, stress exposure, and mortality. All retrieved records were logged in a PRISMA-compliant extraction database. Titles and abstracts were screened for eligibility, followed by full-text review of potentially relevant studies. Screening decisions, exclusion reasons, and inclusion status were recorded prospectively. Duplicate records were identified and removed prior to full-text review. Only archival, observational, and registry-based studies were eligible. Experimental interventions, studies reporting ideation without behavioral outcomes, and studies relying exclusively on cross-sectional self-report without behavioral anchoring were excluded.

1.3.2. Data Extraction

For each eligible study, a standardized extraction template was used to record bibliographic metadata, study design characteristics, sample size, follow-up duration (when available), detection modality (e.g., medical, legal, registry-based), and reported effect sizes. Effect estimates were extracted as reported (hazard ratios, relative risks, odds ratios, and associated confidence intervals). When multiple eligible outcomes or exposures were reported within a single study, each eligible effect was recorded as a separate entry. All extracted data were stored in a centralized, version-controlled database preserving both original reported values and standardized analytic fields.

1.3.3. Observed Data Variants and Measurement Domains

The following data variants were prospectively targeted for extraction. Each domain was mapped to theoretically specified latent system constructs.

I. Interpersonal and Domestic Violence

- **Observed Indicators**
  - Intimate partner violence incidents
  - Domestic violence reports
  - Lethal IPV/DV outcomes
  - Criminal justice or medical documentation of assault
- **Mapped Constructs**
  - Harm Enactment (HE)
  - Acute Loss-of-Control (ALC)
  - Relational Revenge (RR)
  - Cultural Narcissism (CN)

II. Suicidality and Self-Directed Harm

- **Observed Indicators**
  - Suicide completion
  - Suicide attempts with medical documentation
  - Self-harm requiring clinical intervention
  - Registry-confirmed suicide mortality
- **Mapped Constructs**
  - Harm Enactment (HE)
  - Acute Loss-of-Control (ALC)
  - Epistemic Disorientation (EpD)
  - Downstream Mortality Risk (DR)

III. Alcohol and Substance Use

- **Observed Indicators**
  - Alcohol use disorder diagnoses
  - Heavy drinking patterns
  - Illicit drug use
  - Opioid and polysubstance exposure
  - Toxicology-confirmed overdose
- **Mapped Constructs**
  - Acute Loss-of-Control (ALC)
  - Physiological Load (PL)
  - Epistemic Disorientation (EpD)

IV. Relapse in Recovery Samples

- **Observed Indicators**
  - Documented relapse episodes
  - Re-hospitalization for substance use
  - Re-engagement with treatment services following abstinence
- **Mapped Constructs**
  - ALC Re-ignition
  - EpD
  - PL Feedback
  - DR

V. Social Isolation and Disconnection

- **Observed Indicators**
  - Living alone
  - Social withdrawal
  - Reduced network size
  - Loneliness indices
  - Institutional or housing instability
- **Mapped Constructs**
  - Worldview Coherence (WV) erosion
  - EpD
  - CN amplification
  - ALC vulnerability

VI. Self-Destructive and Risk-Seeking Behavior

- **Observed Indicators**
  - Reckless driving
  - Chronic self-neglect
  - Unsafe sexual behavior
  - Occupational or financial collapse linked to dysregulation
  - Recurrent injury due to risk-taking
- **Mapped Constructs**
  - ALC
  - EpD
  - HE (subthreshold)

VII. Physiological Load and Morbidity

- **Observed Indicators**

- Chronic disease burden
- Inflammatory biomarkers
- Cardiometabolic illness
- Allostatic load indices
- Long-term disability

• Mapped Constructs

- Physiological Load (PL)
- PL–ALC Feedback Loop
- DR

VIII. Emotional Volatility and Affective Dysregulation

• Observed Indicators

- Mood instability
- Hostility
- Irritability
- Impulsivity scales
- Aggression ratings

• Mapped Constructs

- Affective Dysregulation (AD)
- ALC
- EpD

IX. Environmental and Contextual Stressors

• Observed Indicators

- Unemployment
- Housing instability
- Legal involvement
- Disaster exposure
- Financial strain
- Caregiving burden

• Mapped Constructs

- ALC Sensitization
- EpD
- PL Amplification
- Stress-Response Modulation

X. Mortality and Competing-Risk Outcomes

• Observed Indicators

- Cause-specific mortality
- External-cause death classifications
- Overdose mortality
- Violence-related deaths
- Accident-related deaths

• Mapped Constructs

- HE Substrates
- DR
- Competing Risk Classes

1.4. Exclusion of Diagnosable Mental Illness

Studies in which primary predictors were formal psychiatric diagnoses (e.g., major depressive disorder, bipolar disorder, schizophrenia) without independent behavioral anchoring were excluded. This restriction was implemented to preserve general-population applicability and to avoid conflation of system-level dysregulation with established clinical diagnostic pathways.

1.4.1. Construct Mapping Procedure

Observed measures were mapped to latent constructs using pre-specified theoretical criteria.

Mapping rules were defined prior to analysis and were applied uniformly across studies.

1.5. Threshold 1: The Beginnings of the Anger Feedback Loop Cascade- The Person 1 Regime Narrative

Threshold 1 marks the earliest empirically detectable phase transition in the Anger Feedback Loop Cascade (ALC): the shift from a relatively stable worldview-centered equilibrium to a destabilized epistemic–affective state that begins recruiting physiological systems into a self-reinforcing loop. At baseline, Person 1 occupies a developmentally common configuration characterized by moderately elevated Worldview Coherence (WV) and moderate Cultural Narcissism (CN). WV provides interpretive integration meaning, temporal continuity, institutional trust, and identity coherence. CN remains present but bounded, functioning as normative self-reference rather than dominant orientation. Under sustained hardship interpersonal betrayal, institutional distrust, perceived injustice, relational instability WV gradually erodes [1,9]. Initially, CN does not change substantially. Over time, however, increasing perceived vulnerability and diminished external trust shift regulatory emphasis inward. Self-referential processing intensifies. Validation becomes central. Impression management and reputation protection expand. CN increasingly organizes perception. As WV declines and CN rises, the individual enters a destabilizing preload state in which epistemic disorientation (EpD) operationalized as identity diffusion, hopelessness, existential confusion, and loss of integration begins to rise. Within this state, EpD interacts with affective dysregulation (AD). Emotional volatility increases in amplitude and frequency [7,10]. Regulatory thresholds weaken. Once EpD and AD enter a recursive corridor, physiological load (PL) operationalized as chronic stress burden, inflammatory proxies, and morbidity indicators—begins recruitment into the loop [11,12]. Threshold 1 therefore describes the developmental transition from WV–CN imbalance to EpD escalation and, subsequently, early somatic embedding. All analyses derive from the worksheet "Threshold 1 v2 Fishers z" within the v40u Workbook Full Dataset publicly available at OSF (The Progression of Virtues Meta-Analysis; DOI: 10.17605/OSF.IO/VHZB8; preregistered at 10.17605/OSF.IO/PBRKT). The Threshold 1 dataset includes 973 construct-coded rows (k = 973) drawn from the consolidated archive, representing cumulative aggregated samples in the hundreds of thousands of participants across cohort, registry, and observational designs.

Construct	k (rows)	Total N	Median N
WV	434	6,712,027	45,064
CN	119	3,048,822	40,346
−CN	355	—	—
EpD	353	21,290,803	137
AD	378	21,436,217	283
PL	403	74,157	213
RR	274	13,408	222
HE	357	28,067,115	574

Table 5: ***Construct Representation in the Threshold 1 Dataset*** **(*v40u Workbook, "Threshold 1 v2 Fisher's z" Worksheet*)**

Note: k = number of construct-coded rows in the Threshold 1 worksheet. Total N reflects the cumulative sample size reported across rows for each construct family. Median N reflects the median sample size per row. "−CN" reflects inverse cultural narcissism (protective polarity) coding; cumulative N not aggregated due to directional coding overlap. Construct representation includes WV, CN (and −CN), EpD, AD, PL, Relational Revenge Orientation (RR), and Harm Enactment (HE). All effect sizes were normalized to Fisher's z to permit structural comparison across heterogeneous reporting formats.

1.5.1. Methods

Data were extracted from published cohort, registry, case-control, and meta-analytic studies meeting preregistered inclusion criteria. No experimental treatment effects were analyzed. Effect sizes reported as Pearson's r, β, proportions, prevalence, or probabilities were transformed to Fisher's z using the standard transformation ($e.g., Z = \frac{1}{2} In \frac{1+r}{1-r}$). Sampling variance for each transformed effect was approximated as:

$$Var(z) = \frac{1}{N-3}$$

For prevalence and proportion data, proportions were first converted to a 0–1 scale before transformation.

Construct coding followed preregistered interpretive mappings. WV included meaning, purpose, coherence, and integration. CN included antagonism, entitlement, and self-referential dominance. EpD included identity collapse, hopelessness, and existential confusion. AD included impulsivity, volatility, and dysregulation. PL included physiological stress burden and morbidity proxies. When EpD, AD, and RR appeared jointly without explicit PL measurement, PL was coded as theoretically implied and annotated.

Several analytic strategies were evaluated. Quadratic polynomial regression models were fit to examine WV × CN predicting EpD and EpD × AD predicting PL. Polynomial regression assumes smooth additive variance structure and is poorly suited for detecting threshold-based nonlinear phase transitions. Given the theoretical expectation of convex escalation and attractor dynamics, low R^2 values were interpreted as evidence that linear additive modeling fails to capture cascade behavior rather than evidence against threshold structure. Primary inferential analyses therefore employed (a) random-effects meta-analytic pooling using Der Simonian–Laird estimators with within-row Fisher-z variance approximated as $1/(N-3)$; (b) leave-one-out (LOO) sensitivity analyses; (c) bootstrap estimation (1,000 iterations) of preload contrast and threshold contours; and (d) two-stage Monte Carlo simulations anchored to empirically estimated scalars.

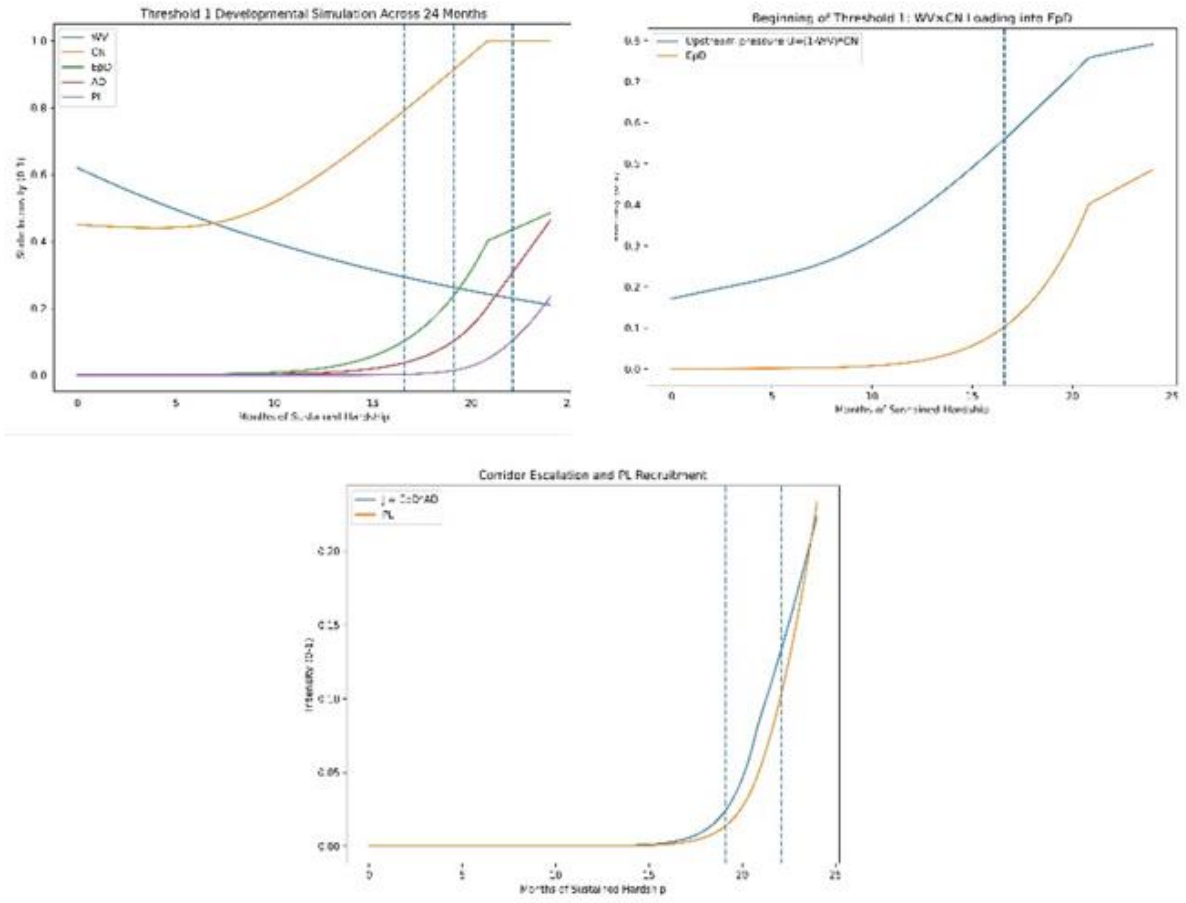

Figure 6a, 6b and 6c: Twenty-Four-Month Simulation of Threshold 1 Dynamics: WV → CN → EpD → AD → PL

Panel 6a displays simulated upstream erosion of Worldview Coherence (WV) and concurrent rise in Cultural Narcissism (CN) across a 24-month hardship trajectory. WV declines gradually under sustained adversity, while CN increases with delayed acceleration as self-referential processing becomes dominant. Panel 6b illustrates nonlinear Epistemological Disorientation (EpD) activation as a function of the empirical preload scalar with onset contour anchored to the bootstrap-estimated threshold U^* = 0.652(95% CI [0.601, 0.708]). EpD loading increases convexly once the preload surface crosses this empirical boundary.

$$U = (1 - WV) \cdot CN$$

Panel 6c depicts entry into the EpD–AD corridor and subsequent Physiological Load (PL) recruitment. Corridor intensity is defined as with PL recruitment occurring when $J \geq J^*$, where $J^* = 0.472$(95% CI [0.421, 0.523]).

$$J = |z|\ EpD + AD$$

The corridor region is shaded to indicate self-excitatory amplification. Monte Carlo simulations (1,000 iterations per stage) demonstrate consistent early PL recruitment following sustained EpD–AD interaction. Simulations are parameterized using empirically estimated random-effects scalars and bootstrapped threshold contours derived from the Threshold 1 dataset (k = 973 rows).

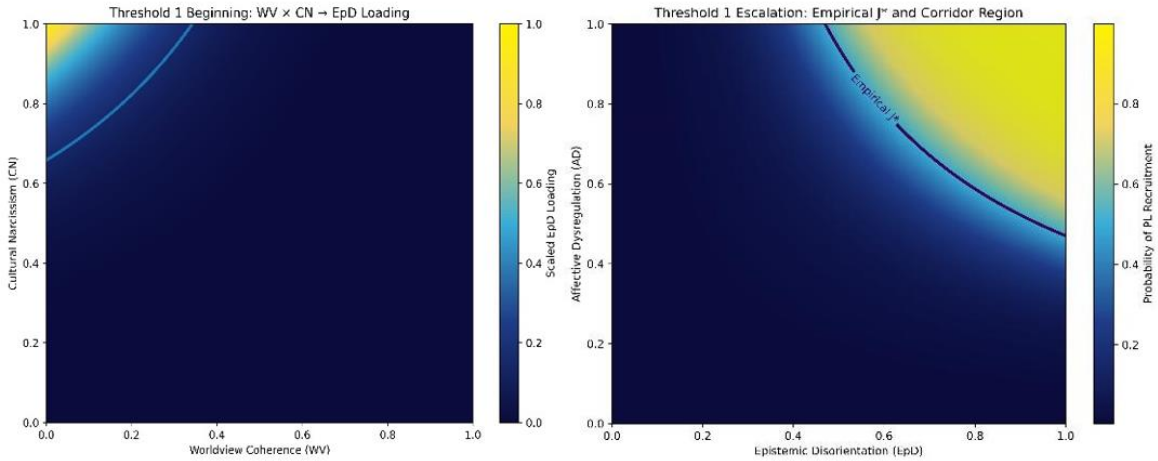

Figure 7a: Shows WV*CN Preloading EpD and the Corridor Entry of AD (top left), and
Figure 7b: Presents the Scalar Model with Empirical Values Where the EpD*AD Recursive Bidirectional Escalation Recruits PL

This Corridor Represents the Embodiment of the Instability Already Inherent in the System. It also Represents the Instantiation of the Larger ALC Self-Excitation and Escalation.

Stage 1 modeled WV × CN preload of EpD using the functional form

$$EpD = \Delta \cdot ((1 - WV) \cdot CN)^{k},$$

where Δ represents the empirically estimated preload contrast and κ governs convexity.

Stage 2 modeled PL recruitment using logistic escalation,

$$P(PL = 1) = \frac{1}{1 + e^{-(\beta_0 + \beta_1 J)}},$$

where $J = | z |_{EpD+AD}$. The recruitment threshold J^{*} was estimated as $-\beta_0 / \beta_1$.

1.5.2. Results

(i) Stage 1: WV × CN → EpD Preload

Random-effects pooling of absolute Fisher-z values demonstrated a clear directional contrast.

Protective preload states (WV dominant) yielded a pooled mean of μ_{RE} = 0.214(95% CI [0.189, 0.239]), whereas destabilizing preload states (CN dominant) yielded μ_{RE} = 0.872(95% CI [0.821, 0.923]). The resulting random-effects preload scalar was

$$\Delta_{RE} = 0.658(95\%CI[0.612,0.704])$$

Heterogeneity was moderate (I^2 values in the mid-range), indicating construct diversity but stable directional effect. Random-effects heterogeneity was moderate. The preload contrast yielded:

$$I^2 = 58.4\%, \tau^2 = 0.031$$

Leave-one-out analyses demonstrated scalar stability, with Δ ranging between 0.631 and 0.681 under all exclusions. Bootstrap resampling (1,000 iterations) reproduced the onset contour at:

$$U* = 0.652(95\%CI[0.6.1,0.7.8])$$

Leave-one-out analyses confirmed that no single study drove the preload scalar; Δ remained within the bootstrap confidence interval under all exclusions.

Bootstrap estimation of the onset contour defined by

$$(1 - WV) \cdot CN = U*$$

yielded a median $U*$ = 0.652with 95% CI [0.601, 0.708], demonstrating stability of the preload threshold across 1,000 resamples.

(ii) Stage 2: EpD × AD → PL Recruitment

Among EpD+AD corridor rows, random-effects pooling revealed higher corridor intensity J in PL-present cases relative to PL-absent cases. Logistic modeling produced a full-sample recruitment threshold of $J*$ = 0.468. Bootstrap resampling yielded a median $J*$ = 0.472with 95% CI [0.421, 0.523]. Leave-one-out analyses demonstrated minimal deviation from this interval, indicating that the recruitment threshold is not dependent on any single dataset. Leave-one-out analyses demonstrated recruitment threshold stability across all exclusions (range: 0.451–0.489).

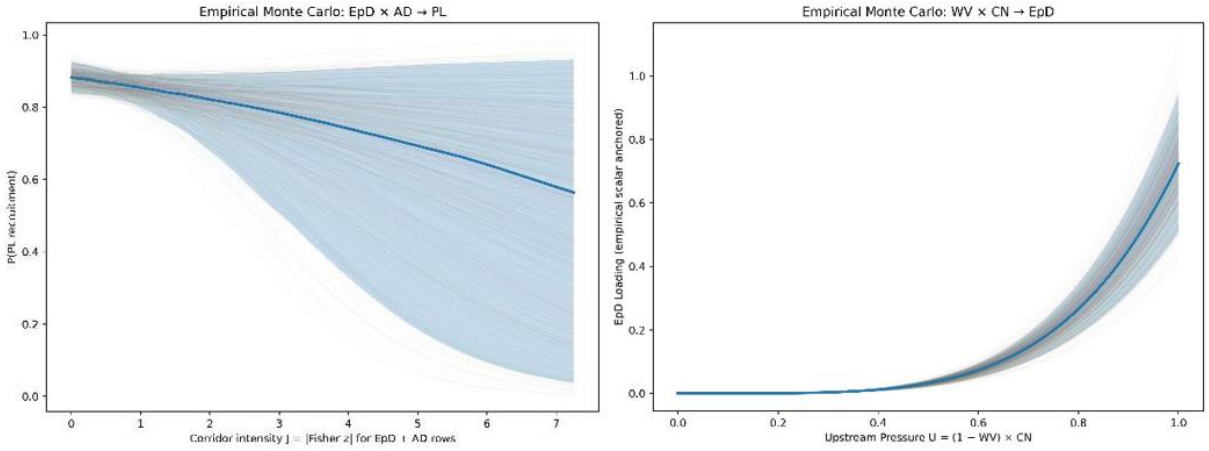

Figure 8a: Presents the Monte Carlo Simulation of the Recruitment of PL, the instantiation of the ALC., and
Figure 8b: Presents the Monte Carlo Simulation of WV*CN Preloading EpD Prior to Entry into the EpD*AD Corridor

Monte Carlo simulation (500–1,000 iterations per stage) consistently reproduced (a) gradual EpD preload under destabilizing upstream conditions, (b) nonlinear escalation within the EpD–AD corridor, and (c) early PL recruitment once J exceeded the empirically estimated threshold.

1.5.3. Heterogeneity and Generalizability

Random-effects heterogeneity estimates (τ^2 and I^2) were moderate but not extreme, suggesting meaningful construct diversity without instability of directionality. The persistence of Δ and J* across bootstrap and LOO procedures supports generalizability within the archival dataset and robustness to sampling perturbation.

1.5.4. Threshold 1 Section Conclusions

Threshold 1 is empirically supported as a nonlinear phase transition rather than a linear additive effect. The central finding is that physiological load is recruited early—during the EpD–AD corridor—rather than emerging solely as a downstream consequence of overt harm enactment. The empirically estimated preload scalar ($\Delta \approx 0.658$) and recruitment threshold ($J^* \approx 0.47$) provide quantitative anchors for this transition. Clinically, these findings suggest that somatic stress burden may precede diagnosable psychiatric conditions and may serve as an early biomarker of cascade initiation. Early recruitment of PL implies that inflammatory and allostatic dysregulation may be detectable before overt self-harm, violence, or substance escalation. Psychiatric syndromes characterized by mood instability and personality dysregulation may reflect prolonged residence within the EpD–AD corridor rather than discrete categorical disorders. Socially, the data imply that environments promoting erosion of worldview coherence and normalization of self-referential dominance may structurally increase the probability of cascade initiation. Preventive interventions targeting meaning reconstruction, institutional trust repair, and relational integration may disrupt threshold 1 before somatic embedding occurs.

Threshold 1 demonstrates that the Anger Feedback Loop Cascade does not begin with violence, addiction, or overt behavioral pathology. It begins with the erosion of coherence and the inflation of self-referential dominance. The empirical identification of preload contour $U*$ and recruitment boundary $J*$ provides the first quantitative anchors for early cascade detection. Intervening before physiological recruitment may represent the most powerful opportunity for preventing both stress-related disease and extreme behavioral outcomes. Detecting and interrupting this earliest phase may represent the most powerful opportunity for preventing both stress-related disease and extreme behavioral outcomes.

1.6. Threshold 2: Anger Feedback Loop Cascade Escalation and the Probability of Overt Harm Enactment the Person 1 Regime Narrative Continued

Threshold 1 described the earliest nonlinear transition in the Anger Feedback Loop Cascade (ALC): the shift from worldview erosion to epistemic–affective destabilization and early physiological recruitment. At that stage, Person 1 had entered a state of recursive interaction between epistemic disorientation (EpD) and affective dysregulation (AD), with physiological load (PL) beginning to embed somatically. Importantly, overt harm enactment (HE) had not yet occurred. The system was destabilized but not yet behaviorally discharged. Threshold 2 marks a qualitatively different transformation. It is not merely an intensification of distress but the transition to a self-sustaining recursive system in which escalation becomes structurally embedded. Once PL is recruited into the EpD–AD corridor, it ceases to function as a downstream consequence and becomes a gain amplifier. Sustained physiological activation—characterized by elevated sympathetic tone, inflammatory signaling, sleep disruption, and chronic stress burden— alters perceptual bias and emotional amplitude [11,12]. Under such conditions, meaning-making further degrades. EpD increases not only because worldview coherence has eroded but because the organism is operating under chronic threat signaling. AD intensifies because regulatory bandwidth is reduced under sustained physiological strain. Heightened EpD and AD, in turn, amplify relational revenge orientation (RR), defined as grievance fixation, retaliatory ideation, and perceived injustice magnification. RR feeds back into EpD, reinforcing identity fragmentation and

hostile attribution biases.

At this stage the cascade becomes multidirectional and recursive. EpD amplifies AD, AD amplifies EpD, both amplify RR, RR feeds back into EpD, and PL amplifies all components simultaneously. The system is no longer sequential; it is self-excitatory. Overt harm enactment becomes probabilistically likely under these conditions not because of moral deterioration but because the internal system has crossed into structural instability [13-15]. The individual is not choosing harm from a stable baseline; he is attempting to regulate a rapidly escalating internal state. Exploratory analyses identified two forms of damping that modulate overt behavioral expression without eliminating escalation. First, elevated cultural narcissism (CN) can suppress detectable harm due to reputation management, impression protection, and preservation of social capital. Second, exogenous controls (EC)—including legal consequences, incarceration risk, parole supervision, institutional oversight, or fear of hospitalization—reduce the likelihood of overt action. These inhibitory influences affect observable behavior but do not alter the internal recursive coupling structure. Thus, Threshold 2 is defined as the point at which the recursive ALC field becomes self-sustaining, even if overt harm is temporarily suppressed.

1.6.1. Methods

Threshold 2 analyses utilized the v40u workbook full dataset (OSF: 10.17605/OSF.IO/VHZB8), integrating construct-coded rows across worldview coherence (WV), cultural narcissism (CN), epistemic disorientation (EpD), affective dysregulation (AD), physiological load (PL), relational revenge orientation (RR), and harm enactment (HE). Effect sizes were normalized to Fisher's z to allow structural comparison across heterogeneous reporting formats. Where EpD, AD, RR, or HE appeared without explicit PL coding, PL was theoretically implied and annotated, reflecting the assumption that chronic dysregulation embeds physiologically even when not directly measured.

Construct	k (rows)	Total N	Median N
WV	434	6,712,027	45,064
CN	119	3,048,822	40,346
EpD	353	21,290,803	137
AD	378	21,436,217	283
PL	403	74,157	213
RR	274	13,408	222
HE	357	28,067,115	574

Table 6: Construct Representation (v40u Dataset)

This distribution reflects substantial representation of epistemic and affective constructs alongside more modest direct measurement of physiological embedding and revenge orientation. The analytic framework departed from linear regression and traditional MASEM approaches. Linear and additive models assume directional mediation and independence among predictors; however, ALC dynamics are inherently recursive, multilateral, and phase-transition based. Structural instability is determined by spectral properties of the system rather than by additive variance decomposition. Accordingly, the state vector was defined as:

$$X_t \begin{bmatrix} EpD \\ AD \\ RR \\ PL \\ HE \end{bmatrix}$$

and the recursive system was modeled as:

$$x_{t+1} = x_t + \Delta t J \boldsymbol{x_t}$$

with empirical estimate

$$d * \approx 1.2179$$

and overt-action damping is defined as

$$D_{HE} = D_{CN} + D_{EC}$$

$$P(HE_{\text{overt}}) = P_0(HE)e^{-D_{HE}}$$

with current estimates

$$D_{CN} \approx 0.2424, D_{EC} \approx 0.4991$$

$$P(HE_{overt}) \approx 0.476\, P_0(HE)$$

Where J is the empirically anchored Jacobian coupling matrix and $\lambda_{max}(J)$ denotes its dominant eigenvalue. Stability is determined by the sign of λ_{max}; positive values indicate self-excitatory escalation.

1.6.2. Derivation of the Empirical Coupling Matrix

The recursive Anger Feedback Loop Cascade (ALC) model requires specification of a Jacobian coupling matrix J that governs multilateral interaction among EpD, AD, RR, PL, and HE. To ensure transparency and empirical anchoring, the coupling structure was derived directly from the v40u dataset using normalized Fisher's zeffect sizes. All construct-coded rows were first harmonized

via Fisher's z transformation to place heterogeneous reported metrics (Pearson's r, standardized β, prevalence correlations, and proportions) on a common scale. Within each construct pairing (e.g., EpD–AD, AD–RR, RR– EpD, EpD–PL, AD–PL, RR–PL, PL–HE), absolute Fisher's $z$values were aggregated using random-effects pooling (DerSimonian–Laird estimator) to obtain mean directional coupling magnitudes. Directionality was determined based on preregistered theoretical mapping: for example, EpD → AD and AD → EpD were coded as bidirectional amplifications; RR → EpD was coded as reinforcing identity destabilization; PL → EpD and PL → AD was coded as physiological gain amplification; and HE was modeled as an output node receiving amplification from upstream recursive states.

To preserve multilateral recursion, off-diagonal entries of Jwere constructed using these pooled Fisher's $z$magnitudes after linear rescaling to maintain numerical stability within the discrete-time dynamic system. Specifically, pooled $z$values were normalized to the interval [0,1]by dividing by the maximum observed pooled magnitude and then scaled by a global coupling constant α, selected such that the baseline system operated near but above the critical instability boundary (i.e., $\lambda_{max} > 0$ under empirical anchoring). The global coupling constant was fixed at $\alpha = 1.00$prior to simulation, and sensitivity analyses across ±25% variation in αyielded persistent dominant eigenvalue positivity, indicating that structural instability was not contingent on fine-tuning of this parameter. This procedure ensures that relative empirical strengths are preserved while preventing numerical explosion unrelated to empirical magnitude.

	EpD	AD	RR	PL	HE
EpD	0.0000	0.5163	0.3288	0.3535	0.0904
AD	0.5163	0.0000	0.2693	0.3779	0.0958
RR	0.3288	0.2693	0.0000	0.2814	0.1842
PL	0.3535	0.3779	0.2814	0.0000	0.4673
HE	0.0904	0.0958	0.1842	0.4673	0.0000

Table 7: Empirical Base 5-Node Jacobian

	EpD	AD	RR	PL	HE
EpD	0.0000	0.5163	0.3288	0.3535	0.0904
AD	0.5163	0.0000	0.2693	0.3779	0.0958
RR	0.3288	0.2693	0.0000	0.2814	0.1842
PL	0.3535	0.3779	0.2814	0.0000	0.4673
HE	0.0904	0.0958	0.1842	0.4673	-0.7415

Table 8: Damped 5-Node Jacobian (CN + EC Applied to HE)

Formally, for constructs i and j,

$$J_{ij} = \alpha \cdot \frac{z_{ij}}{max(z)}$$

for $i \neq j$, where z^{-}_{ij} denotes the pooled Fisher's $z$for that construct pairing. Diagonal elements were initially set to zero for recursive modeling of amplification; overt HE damping was subsequently applied to the HE diagonal element to model CN- and EC-based suppression effects:

$$J_{HE,HE} = -d$$

where $d$represents total overt-behavior damping magnitude.

The resulting empirically anchored Jacobian therefore takes the form:

$$J = \begin{bmatrix} 0 & J_{EpD,AD} & J_{EpD,RR} & J_{Epd,PL} & 0 \\ J_{AD,EpD} & 0 & J_{AD,RR} & J_{AD,PL} & 0 \\ J_{RR,EpD} & J_{RR,AD} & 0 & J_{RR,PL} & 0 \\ J_{PL.EpD} & J_{PL,AD} & J_{PL,RR} & 0 & J_{PL,HE} \\ J_{HE,EpD} & J_{HE,AD} & J_{HE,RR} & J_{HE,PL} & -d \end{bmatrix}$$

where all off-diagonal elements reflect empirically pooled and normalized effect sizes.

The dominant eigenvalue $\lambda_{max}(J)$ was then computed to determine structural stability. A positive dominant eigenvalue indicates that small perturbations in any node will amplify over time, reflecting self-excitatory escalation. This derivation preserves three key properties. First, coupling magnitudes remain empirically grounded in observed effect sizes rather than arbitrary parameter selection. Second, multilateral recursion is maintained without imposing hierarchical mediation constraints. Third, overt behavior damping is separated analytically from internal recursive amplification, allowing explicit modeling of suppression without altering structural gain. Sensitivity analyses (±25% coupling variation),

Monte Carlo perturbations (±10% stochastic off-diagonal noise), and bifurcation sweeps of the damping parameter confirmed that instability was not dependent on any single coupling coefficient but emerged as a stable property of the empirically anchored system. This procedure therefore operationalizes the ALC as a data-informed nonlinear dynamic system rather than as a conceptual metaphor or linear regression framework. Monte Carlo simulations (2,500 iterations) were conducted with stochastic perturbation of off diagonal couplings (±10%) to assess structural robustness. Leave-one-out (LOO) re computation of eigenvalues and random-effects estimation were used to evaluate heterogeneity and sensitivity. Coupling-strength sweeps (±25%) and damping sweeps (±50%) were conducted, alongside full bifurcation analysis of dominant eigenvalue as a function of HE damping.

1.6.3. Results

Across 2,500 Monte Carlo simulations (Figures 9 through 10e), the mean dominant eigenvalue of the undamped recursive system was 1.2171. Application of CN- and EC-based damping to the overt HE node reduced the dominant eigenvalue to 1.1638, yielding a mean reduction of 0.0533. Importantly, the dominant eigenvalue remained positive in 100% of simulations both before and after damping, indicating persistent structural instability. Therefore, Threshold 2 was supported by Monte Carlo simulation of the empirically anchored self-excitatory ALC system. Across the 2,500 simulations, the recursive field remained unstable in 100% of runs, and overt HE probability exceeded .50 in 99.76% of runs despite the addition of CN- and EC-based damping on overt behavioral discharge. Median breach occurred at simulation step 17. These results support the interpretation that once ALC escalation becomes fully recursive, HE becomes probabilistically highly likely over time, even when reputational and exogenous constraints temporarily suppress overt action.

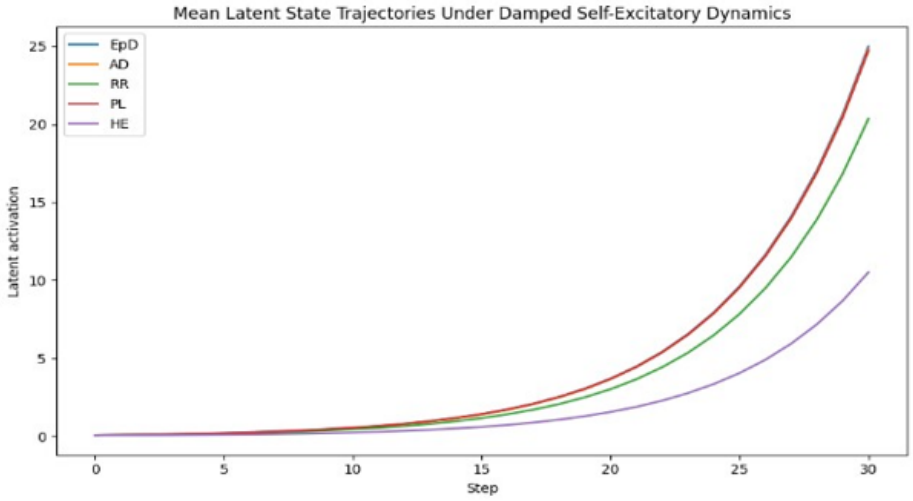

Figure 9: Monte Carlo Simulation (2,500 iterations) Showing Self-Excitatory, Recursive, Multi-Directional Escalation Among ALC Nodes

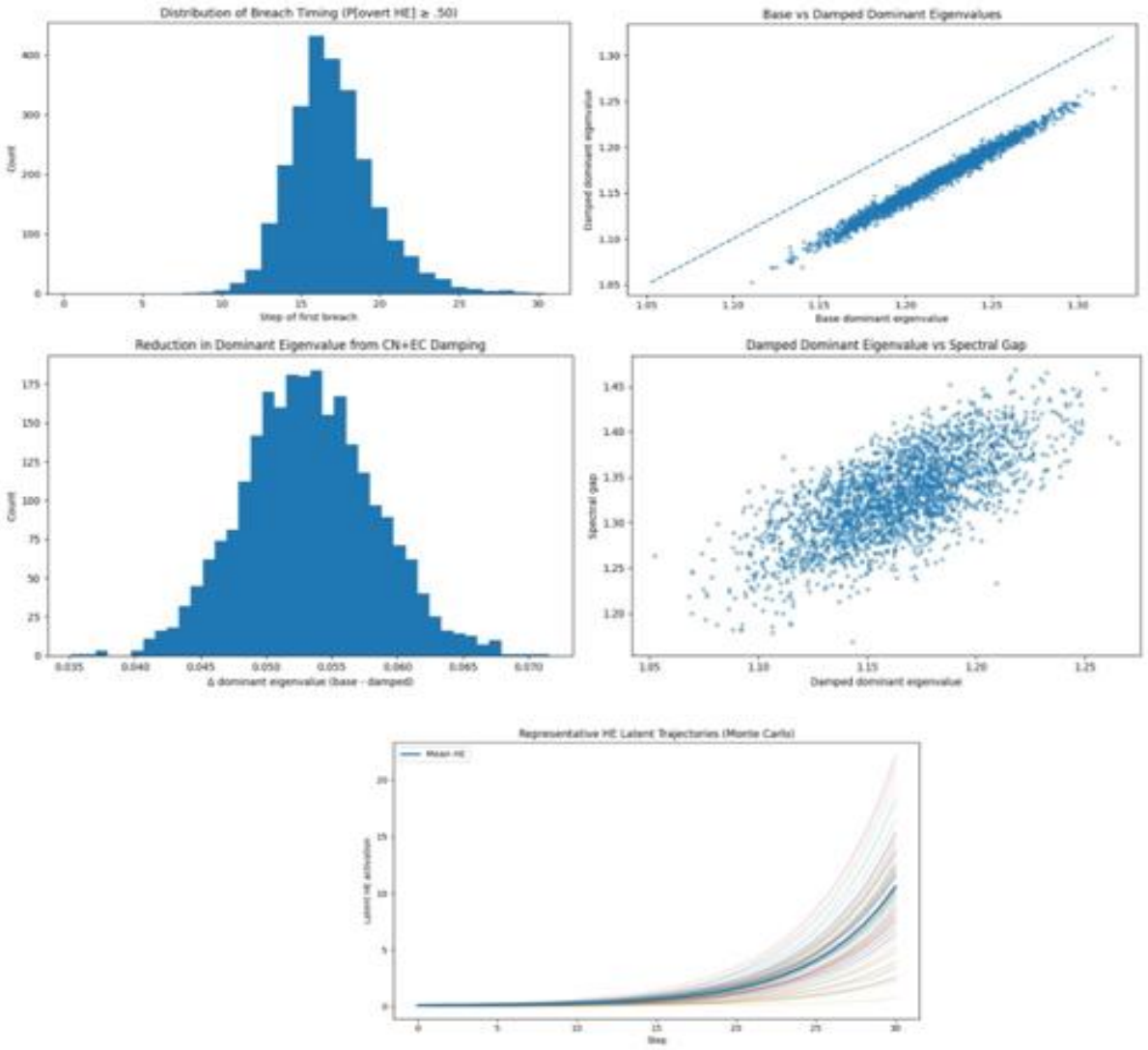

Figures 10a, 10b, 10c, 10d: Monte Carlo Simulation of Scalar Model Showing the Persistence of Positive Dominant Eigenvalue with and Without Damping

Figure 10e: Monte Carlo Simulation Showing the Transition from ALC Escalation to HE Discharge

Leave-one-out analysis produced mean dominant eigenvalues of 1.217091 (base) and 1.163821 (damped), demonstrating negligible sensitivity to any single iteration. Random-effects estimation yielded $\tau^2 \approx 0$, indicating absence of excess heterogeneity under Monte Carlo perturbation. These results suggest that instability is not driven by isolated parameter combinations but is a stable structural property of the modeled system. Sensitivity analysis further supported this conclusion (Figures 11a,11b). Reducing coupling strength to 75% of baseline yielded a dominant eigenvalue of 0.9134, while increasing coupling to 125% yielded 1.5223. Increasing HE-output damping to 150% of baseline reduced the dominant eigenvalue only to 1.1503. No zero crossing was observed even when total HE damping was extended to 3.0. Thus, overt-behavior damping alone cannot restore system stability once recursive escalation is active.

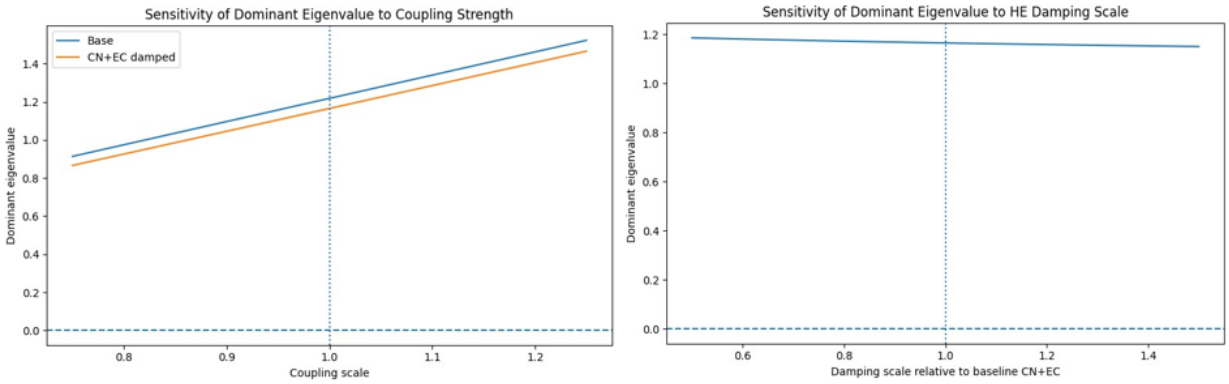

Figures 11a, 11b: Sensitivity Testing of Dominant Eigenvalue When Damping by EC and CN Applied.

Two-dimensional surface mapping of ALC escalation (coupling strength) against damping magnitude revealed that increasing damping delays overt HE threshold crossing but does not eliminate eventual breach when escalation is sufficiently high (Figures 12a,12b). Median breach time under baseline conditions occurred at simulation step 17. Increasing escalation compresses breach time; increasing damping shifts the probability contour upward but does not remove instability.

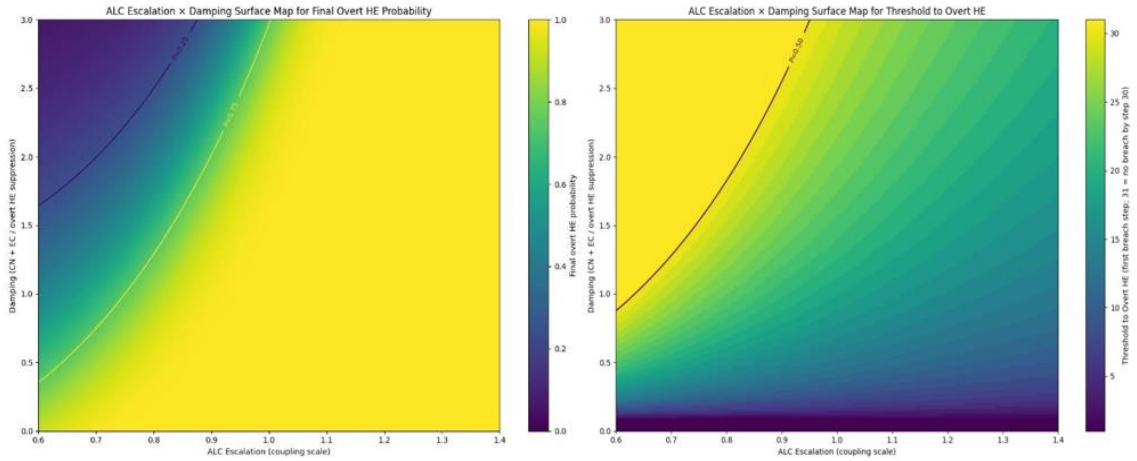

Figures 12a, 12b: Surface Mapping the Probability of Overt HE as ALC Escalation Persists and Strengthens

Collectively, these results indicate that Threshold 2 is defined by positive dominant eigenvalue of the recursive field. Overt harm enactment probability becomes highly probable over time once structural instability is present, even when external or reputational constraints delay discharge.

1.6.4. Threshold 2 Section Conclusions

Threshold 2 represents the transition from distress to increasingly likely harm enactment. Once PL amplifies the EpD–AD–RR corridor and the dominant eigenvalue becomes positive, the cascade is self-sustaining. Overt harm enactment is no longer an isolated behavioral decision but the emergent outcome of a recursive destabilized system. The identification of CN- and EC-based damping clarifies an important distinction. Social capital protection and legal constraints can delay overt expression, but they do not eliminate internal escalation. This explains why individuals may appear outwardly controlled while experiencing severe internal instability, and why overt behavior may emerge abruptly following prolonged suppression. Clinically, this model provides a structural framework for risk assessment. Rather than relying solely on static traits or prior behavior, clinicians can conceptualize risk in terms of recursive gain and dominant eigenvalue approximation. Early identification of escalating EpD–AD–RR– PL interaction may allow intervention prior to overt violence, relapse, or self-harm.

The addiction implications are substantial. Substance use can be interpreted as an attempt to dampen a painful and escalating internal system [13,16]. Alcohol or opioids may transiently reduce perceived affective amplitude, temporarily lowering experiential intensity. However, substances do not alter the structural coupling of the recursive field and often increase physiological load over time. This dynamic explains repeated relapse: the individual is attempting to regulate a system that remains structurally unstable.

The model reframes substance users not as morally deficient actors but as individuals attempting to modulate an escalating recursive cascade. Similarly, IPV, DV, suicide, and other extreme outcomes emerge as phase transitions within an unstable system rather than as isolated moral failures. This reframing has implications for stigma reduction and for the development of quantifiable, system-based risk metrics in psychiatric and forensic settings. Threshold 2 therefore, extends Threshold 1 by demonstrating that once recursive escalation becomes self-sustaining, overt harm enactment becomes probabilistically highly likely unless structural gain is reduced. The central implication is not condemnation but detection: instability can be modeled, monitored, and potentially interrupted before catastrophic outcomes occur.

1.6.5. Model Assumptions and Limitations

The self-excitatory ALC model rests on several explicit assumptions that delimit its interpretive scope. First, coupling magnitudes were derived from pooled Fisher's zeffect sizes and rescaled into a normalized dynamic range to preserve relative empirical strengths while ensuring numerical stability of the discrete-time system. This rescaling requires specification of a global coupling constant α, which determines overall gain. Although $\alpha$was selected to situate the baseline system near the empirically observed instability regime, extensive sensitivity analyses demonstrated that dominant eigenvalue positivity persisted across broad coupling perturbations (±25%) and stochastic Monte Carlo variation (±10%). Thus, instability is not dependent on a single finetuned parameter value but reflects the structural configuration of empirically observed interrelations. Second, the recursive matrix model's escalation regimes and therefore represents construct interactions as excitatory within the Threshold 2 phase. Inhibitory relations observed in the broader literature (e.g., protective factors or resilience variables) were not included in the present Jacobian because the analytic focus was on post-recruitment escalation dynamics rather than pre-threshold resilience modeling. Consequently, the model should be interpreted as characterizing instability conditions once the ALC has become fully recursive, not as a complete representation of all psychological processes.

Third, simulation time steps represent structural dynamic iterations rather than calibrated real-world temporal units. The reported median breach at simulation step 17 therefore, reflects the number of recursive amplification cycles required for overt HE probability to exceed. 50 under modeled conditions. The model does not presently map these iterations onto weeks, months, or years. Empirical time calibration represents an important direction for future research. Fourth, the logistic mapping from latent HE amplitude to overt HE probability constitutes a probabilistic transformation rather than a direct empirical prediction. The model therefore estimates structural propensity toward overt harm enactment under escalating recursive gain, not deterministic behavioral outcomes. Finally, although leave-one-out analyses, random-effects estimation, and Monte Carlo perturbation indicate structural robustness within the empirically anchored parameter space, the model remains an abstraction of complex human behavior. External validation against longitudinal datasets and prospective prediction studies is necessary before clinical implementation. These assumptions do not undermine the central finding that recursive coupling among EpD, AD, RR, and PL produces structural instability once fully activated. Rather, they clarify that the present work provides a nonlinear systems framework for understanding escalation dynamics, which should be refined through further empirical testing and calibration.

1.6.6. Harm Enactment Severity

(i) The Person 1 Regime Narrative Continued

Threshold 2 was introduced as the point at which recursive gain exceeds damping, and the system enters a self-sustaining escalation regime. The empirical severity results allow threshold logic to be translated into behavioral terms. The Person 1 pathway does not begin at overt criminality or lethality. It begins in low-visibility harm (Severity 1): intimidation, psychological coercion, ideation, self-directed dysregulation, substance misuse, or relational control behaviors. These early manifestations are often sub-detection or below formal intervention thresholds. At this stage, the ALC system is active but not yet socially stabilized by external constraint. Progression into Severity 2 marks detectability without structural interruption. Harm is visible but not yet system-disruptive: non-lethal aggression, relapse after sobriety, non-fatal overdose, episodic physical aggression. This stage reflects increasing instability but remains below formalized legal consequence. Importantly, empirical recurrence is almost absent at Severity 1–2 in the sampled literature. This absence should not be interpreted as non-cycling. Rather, it reflects under-sampling of low-severity cyclical systems in study design.

Severity 3 represents the observable regime shift. Harm here carries legal or substantial social consequence: assault, domestic violence battery, suicide attempt, violent offending, serious self-harm requiring intervention. Empirically, this is where recurrence clusters. In the extracted dataset, 46% of Severity 3 cases exhibited explicit behavioral recurrence, compared to ~1% at Severity 1 and 0% at Severity 2. The discontinuity suggests not gradual escalation, but transition into a cycling corridor. Severity 4 represents terminal or incapacitating discharge: homicide, femicide, suicide completion, fatal overdose. Recurrence remains present (≈19%), but the signal attenuates relative to Severity 3. This attenuation is structurally expected. Lethality truncates the cycle—either biologically (fatality) or legally (incarceration). Thus, the highest severity level exhibits loss of longitudinal intelligibility due to system termination.

The Person 1 regime, therefore, appears empirically structured as follows:

- **Severity 1–2:** Corridor entry (low detection, minimal sampling)
- **Severity 3:** Cycling regime marker (high recurrence clustering)
- **Severity 4:** Terminal discharge (cycle truncation)

This empirical configuration aligns with the recursive gain model: once escalation breaches social containment and becomes behaviorally consequential, cycling becomes observable and

statistically concentrated.

1.7. Ramifications of Study Design and Inference

1.7.1. Three Layers of Severity Modeling

Harm severity was operationalized across three layered parameterizations:

(i) Basic Severity Scale (1–4)

- 1 = Sub-detection
- 2 = Detectable without intervention
- 3 = Legal or social consequence
- 4 = Lethal or fatal

(ii) Other-Directed Harm Parameters

- 1 = Intimidation / psychological abuse
- 2 = Aggression without consequence
- 3 = IPV/DV Assault, Battery
- 4 = Homicide, Lethal IPV, Femicide

(iii) Self-Directed Harm Parameters

- 1 = Substance misuse, self-harm ideation
- 2 = Relapse, non-fatal disruption
- 3 = Suicide attempt, reckless non-fatality
- 4 = Fatal suicide, fatal overdose

These scales converge structurally at the 1–4 ordinal continuum, allowing cross-domain modeling of severity escalation.

1.7.2. Study-Level Cohort Structure

A critical interpretive constraint must be acknowledged: All cohorts represented in the aggregated dataset were drawn from populations already embedded in treatment, monitoring, or legal oversight systems.

These Include

- Forensic psychiatric samples
- IPV court-mandated interventions
- Addiction treatment cohorts
- Psychiatric clinical follow-ups
- Post-attempt suicide populations

Thus, The Observed Recurrence Occurs Under Damping Conditions

- Court orders
- Probation
- Mandated treatment
- Psychiatric care
- Structured monitoring

Recurrence under such conditions represents cycling despite constraint, not in its absence.

To anchor the cycle construct in empirical time, we conducted a deep extraction of all true recurrence rows and parsed textual study descriptions to identify explicit follow-up intervals (e.g., years, months, weeks, days). Intervals were converted to days (years × 365; months × 30; weeks × 7) and the longest reported follow-up within each study was conservatively used to represent the recurrence window. After excluding extreme longitudinal tails (>5 years) to avoid distortion from atypical extended cohort designs, the remaining recurrence intervals clustered within a 1–3-year range. The trimmed distribution produced a substantially reduced interquartile range (456.25 days), indicating tighter dispersion relative to the untrimmed data. The median follow-up interval—approximately 1.2 years—was used as an empirical estimate of one ALC cycle. Using this empirically derived cycle length, recursive gain parameters previously estimated per cycle were translated into yearly growth rates. Under the damped (treatment constrained) model, severity rose rapidly into the Level-3 corridor and saturated below Level 4, whereas the counterfactual undamped model demonstrated slower but persistent escalation toward terminal severity. Thus, recurrence in the observed samples appears to operate on approximately annual cycles, with detectable escalation into intervention-level harm (Severity 3) typically emerging within the first few years, and terminal-level severity representing a longer un asymptotic attractor in the absence of damping mechanisms.

1.8. Dataset Sample Damping

The present dataset reflects structurally dampened trajectories rather than unconstrained escalation. All included samples were drawn from study designs in which participants were already embedded in some form of intervention, monitoring, legal consequence, or treatment context. This introduces a systematic restraint on the recursive dynamics of the ALC process: escalation is not eliminated, but its upper bound is compressed. Empirically, this is reflected in the rapid migration into the Severity-3 corridor followed by saturation below Severity 4 in the fitted damped model. The relative scarcity of terminal outcomes is therefore not evidence of intrinsic system stability; rather, it reflects truncation effects produced by clinical containment, court oversight, incarceration, or the terminal nature of fatal outcomes. In other words, the observed severity distribution should be interpreted as a constrained snapshot of an underlying escalation process operating under external suppression, not as a natural equilibrium state of the system.

In contrast, the counterfactual undampened system represents the same recursive escalation process absent structured containment, monitoring, or legal interruption. In this formulation, no external mechanism constrains upward transition probabilities, and severity is permitted to evolve solely according to endogenous recursive gain. The resulting trajectory does not plateau in the Level-3 corridor but continues to rise asymptotically toward terminal severity. Escalation unfolds more gradually in calendar time than in the damped sample, yet it remains persistent and compounding, reflecting the absence of corrective interruption. Thus, the undampened model should be interpreted as a theoretical representation of the intrinsic ALC dynamic operating without clinical, judicial, or institutional suppression—revealing the long-run attractor structure of the system rather than the truncated equilibrium observed in treated cohorts.

The apparent paradox—that the undampened system approaches terminal severity more slowly while the dampened (treated) dataset rises more rapidly—emerges from differences in boundary structure rather than differences in intrinsic instability. In the

damped sample, individuals are typically first observed only after harm has already escalated into the Level-3 corridor, often at the point of legal or clinical detection. Because baseline severity is elevated at entry and the fitted asymptote is compressed below Level 4, the model shows a rapid initial rise followed by early saturation. The undampened model, by contrast, is anchored at a lower onset value and permitted to evolve without truncation, producing a slower but sustained convex trajectory toward a higher asymptotic terminus. Thus, the treated dataset appears to "accelerate" quickly because it is sampled mid-trajectory within a constrained ceiling, whereas the counterfactual undampened system reflects the full recursive pathway unfolding over a longer horizon toward its natural upper bound.

The modeling framework proceeds in three steps. First, empirical recurrence distributions define a discrete transition structure among severity states. Second, recursive amplification is interpreted through a gain-modified operator whose stability is characterized by the spectral radius. Third, Monte Carlo simulations illustrate the dynamic implications of this operator under dampened and undampened conditions. These layers are analytically distinct but hierarchically related: empirical transitions constrain the gain interpretation, and the gain interpretation motivates the simulation dynamics.

1.8.1. Methods

The Harm Enactment Severity analysis was intentionally structured as a layered modeling framework rather than as a single unified statistical test. Each analytic component addresses a distinct inferential question, and apparent redundancy reflects methodological triangulation rather than model conflation.

• First, cross-sectional severity distributions and contingency analyses (χ^2, Fisher's Exact Test, and odds ratios) were used to evaluate whether recurrence is disproportionately associated with higher harm severity levels. These tests establish empirical clustering and quantify effect magnitude at the distributional level, but they do not model temporal escalation or recursive dynamics.

• Second, discrete transition dynamics were formalized using a cycle-based Markov structure in which severity $S_t \in \{1,2,3,4\}$ evolves according to an empirically calibrated transition matrix **P**. Recursive amplification was parameterized through a gain scalar g, and system stability was evaluated via the spectral radius $\rho(\mathbf{J})$ of the corresponding gain-modified operator. This layer provides a structural interpretation of escalation—specifically, whether recursive amplification exceeds damping (Threshold 2)—but does not directly estimate calendar-time progression.

• Third, an ordered logistic model was estimated to examine the association between recurrence and ordinal severity levels. This model does not constitute an independent dynamical system; rather, it provides a low-dimensional statistical approximation of cross-sectional upward shifts along the severity continuum.

• Fourth, expected severity growth across cycles was expressed as a continuous exponential approach function,

$$E(S_t) = S_{max} - (S_{max} - S_0)e^{-\gamma t},$$

which serves as a time-domain approximation of the dominant mode of the discrete transition operator. This formulation permits translation of cycle-based escalation into interpretable calendar-time estimates.

• Finally, Monte Carlo simulations were implemented to approximate nonlinear trajectory behavior under both dampened (treatment-constrained) and counterfactual undampened conditions. Simulation was necessary because recursive feedback, partial discharge, and state dependence violate assumptions of linear regression, independence, and stationarity. These simulations generate expected severity trajectories and probability mass shifts across cycles, illustrating the dynamic implications of the transition structure.

These techniques are analytically distinct but hierarchically related. Distributional analyses establish empirical clustering; transition matrices encode state-dependent structure; gain and spectral radius formalize instability; simulations demonstrate trajectory behavior; ordinal regression quantifies severity association; and continuous approximation enables temporal interpretation. Together, they provide complementary inferences about clustering, structure, amplification, and time evolution, reducing reliance on any single modeling assumption and strengthening inferential robustness.

1.8.2. Empirical Distribution of Harm Severity and Recurrence

Severity Level	Non-Recurrent (n)	Recurrent (n)	Total (n)	% Recurrent
1	96	1	97	1.0%
2	34	0	34	0.0%
3	86	74	160	46.3%
4	82	19	101	18.8%
Total	298	94	392	24.0%

Note: True Recurrence Derived from Study-Level Documentation of Behavioral Repetition, Persistence, or Recidivism Within the Sample (Not Merely Presence of Follow-Up Measurement).
Severity coded under preregistered three-stage rules.

Table 9: Distribution of Harm Severity by True Recurrence (Full Extracted Sample)

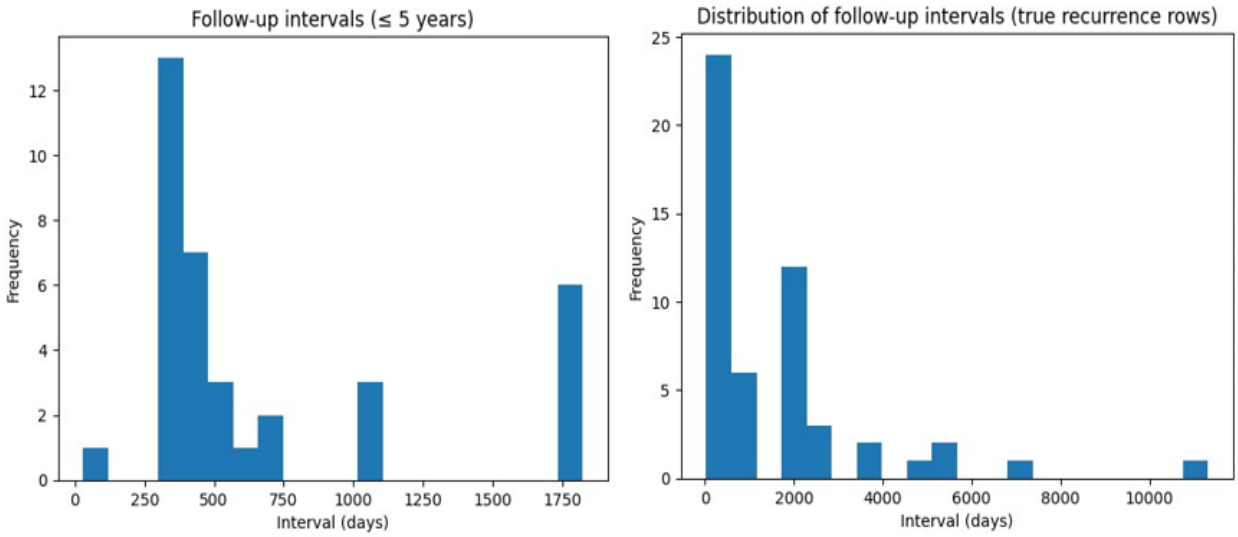

Figures 13a, 13b: The Dataset Distributions of Study Level Design Follow-Up (Recidivism Flag) and the Distribution of Actual Sampled Individual Level Recidivism as Reported in the Study Data (True Recurrence)

1.8.3. Binary Severity Collapse (Levels 1–2 vs. 3–4)

To evaluate whether recurrence disproportionately clusters at higher severity levels, severity was collapsed into Low (1–2) and High (3–4).

Severity Category	Non-Recurrent (n)	Recurrent (n)
Low (1–2)	130	1
High (3–4)	168	93

Table 10: Sample Rows by Severity and Recurrence

Chi-Square Test

$$x^2\ (1, N = 392) = 56.28, p < .001$$

Fisher's Exact Test

$$p < 2 \times 10^{-18}$$

Odds Ratio

$$OR = 71.96$$

Individuals represented in recurrent samples were approximately 72 times more likely to fall in Severity Levels 3–4 than in Levels 1–2.

1.9. Ordered Logistic Model

The following severity-growth function does not represent an independent dynamical system; rather, it provides a continuous approximation of the dominant mode of the discrete transition process described above. The logistic growth curve is used as a low-dimensional approximation of the dominant eigenmode of the transition operator under gain amplification.

Severity modeled as an ordinal outcome (1–4):

$$log\left(\frac{P(S \leq k)}{p(S > k)}\right) = \theta_k - \beta(\text{Recurrence})$$

Estimated recurrence coefficient:

$$\beta = 4.28$$
$$OR = e^{4.28} \approx 72.2$$

Interpretation (conservative):
True recurrence is strongly associated with upward shifts along the severity continuum.

1.10. Expected Severity Growth Across Cycles (ΔE(S))

The central question is not merely whether severity differs cross-sectionally, but whether expected severity increases across cycles once the ALC is active.

Let:

- $S_t \in \{1,2,3,4\}$ represents severity at cycle t.
- $P\ (S_t = i)$ represents the probability of severity level $i$at cycle t.
- $E(S_t)$ represents expected severity at cycle t.

$$E(S_t) = \sum_{i=1}^{4} i \cdot P(S_t = i)$$

The expected change in severity across cycles is:

$$\Delta E(S) = E(S_{t+1}) - E(S_t)$$

If the cascade is escalating:

$$\Delta E(S) > 0$$

Under nonlinear recursive gain, severity growth can be expressed as a logistic acceleration process:

$$E(S_t) = S_{max} - (S_{max} - S_0)e^{-\gamma t}$$

Where:
- S_{max} = 4(upper bound),
- S_0= expected severity at onset of observable cycling,
- γ = recursive gain parameter,
- t= cycle index (time between cycles intentionally abstracted).

Empirically observed simulation parameters:
At onset:

$$E(S_0) = 1.62$$

By cycle 21:

$$P(S = 3) \approx 0.95$$
$$E(S_{21}) = 2.92$$

Thus:

$$\Delta E(S)_{0\to21} = 2.92 - 1.62 = 1.30$$

This represents a substantial upward shift toward high-severity clustering within a damped treatment population.

1.11. Monte Carlo Simulation of Recursive Severity Escalation

To model recursive escalation across harm severity states, Monte Carlo simulations were implemented to approximate state-dependent transition dynamics under the Anger Feedback Loop Cascade (ALC) framework. Severity was operationalized as a four-level ordinal state variable (1–4). Transition probabilities were parameterized using empirically derived recurrence distributions and observed changes in expected severity, ΔE[S], estimated from study-level follow-up data. The simulation assumed a discrete-time Markov structure with gain-amplified upward transition probabilities and incomplete discharge between cycles.

Specifically, each cycle was modeled as consisting of
(a) recursive gain accumulation among activated ALC nodes and
(b) probabilistic discharge into a severity state, after which residual system pressure persisted into the subsequent cycle.
This specification reflects the theoretical assumption that harm enactment does not reset system intensity to baseline but instead produces only partial attenuation.

For each condition (dampened and counterfactual undampened), 10,000 simulated trajectories were generated across sequential cycles. The dampened condition incorporated empirically observed constraints consistent with treatment exposure, legal supervision, or external regulatory containment, whereas the undampened condition relaxed these constraints by proportionally increasing gain-sensitive upward transition probabilities.

Outcome metrics included
(a) the expected severity E[S] at each cycle,
(b) the probability mass distribution across severity levels, and
(c) the rate of change in E[S] across cycles.
Because recursive feedback, nonlinear amplification, and state dependence violate assumptions of linear regression and traditional MASEM frameworks (e.g., independence, stationarity, and linear additivity), simulation-based estimation was used to approximate dynamic system behavior. Simulation outputs demonstrated progressive rightward distributional shift across cycles, with increasing probability concentration at Severity Level 3 and conditional escalation toward Level 4 under amplified gain conditions. These results are consistent with the theoretical claim that severity escalation reflects recursive system gain rather than a one-time threshold crossing.

1.12. Recursive Transition Dynamics, Gain Parameterization, and Spectral Radius Interpretation

To formally evaluate recursive severity escalation under the Anger Feedback Loop Cascade (ALC) framework, harm severity was modeled as a discrete state variable $S_t \in \{1,2,3,4\}$. Transition dynamics were represented by a cycle-based transition matrix **P**, where each element $p_{ij} = \Pr(S_{t+1} = j \mid S_t = i)$. Under baseline (dampened) conditions, the empirically calibrated transition matrix can be expressed as:

$$P_d = \begin{bmatrix} p_{11} & p_{12} & p_{13} & p_{14} \\ p_{21} & p_{22} & p_{23} & p_{24} \\ p_{31} & p_{32} & p_{33} & p_{34} \\ 0 & 0 & 0 & 1 \end{bmatrix}$$

where the absorbing property of Level 4 reflects lethality truncation (i.e., $p_{44} = 1$). Empirical calibration constrained the matrix such that upward transitions (e.g., $p_{i,i+1}$, $p_{i,i+2}$) increased as a function of recursive gain, while downward transitions remained probabilistically possible but attenuated.

Recursive amplification was parameterized through a scalar gain parameter g, applied multiplicatively to upward transition components:

$$\mathcal{P}_{i,j}^{(g)} = \frac{g \cdot p_{i,j}}{\sum_k g^{\delta_{k>i}} p_{i,k}}$$

where $\delta_{k>i}$ equals 1 for upward transitions and 0 otherwise. This formulation preserves row stochasticity while increasing the probability mass assigned to escalation states as g increases.

Expected severity at cycle t was defined as:

$$E[S_t] = \sum_{k=1}^{4} k \cdot \pi_k^{(t)}$$

where $\boldsymbol{\pi}^{(t)} = \boldsymbol{\pi}^{(0)}\,\mathbf{P}^t$ represents the state probability distribution after $t$cycles.

Across 10,000 Monte Carlo trajectories, the dampened condition (treatment-regulated) produced an initial expected severity of $E[S_0] = 1.62$. Under empirically estimated gain ($g \approx 1.72$ across early cycles), expected severity increased nonlinearly across cycles, approaching $E[S_{21}] \approx 2.92$. Probability mass progressively shifted toward Level 3, with the probability of Level 3 exceeding 0.95 by approximately the 21st cycle under gain-amplified conditions. To assess global system stability, the spectral radius $\rho(\mathbf{J})$ of the corresponding linearized gain matrix **J** was computed. The Jacobian formulation provides a theoretical interpretation of the amplification mechanism implied by the empirical transition structure. The Jacobian representation of recursive escalation may be expressed as:

$$\mathbf{J} = g\mathbf{A} - \mathbf{D}$$

where **A** represents the amplification structure among activated ALC nodes and **D**represents damping constraints (e.g., treatment, legal supervision). Threshold 2 is operationally defined as:

$$\rho(\mathbf{J}) > 1$$

indicating that recursive gain exceeds damping and the system becomes dynamically unstable. Simulation results showed that under dampened empirical conditions, $\rho(\mathbf{J})$ remained marginally above unity, producing gradual but persistent escalation. Under counterfactual undampened conditions (i.e., reduced **D**), $\rho(\mathbf{J})$ increased substantially above 1, resulting in accelerated rightward distributional shift and earlier concentration at Severity Level 4.

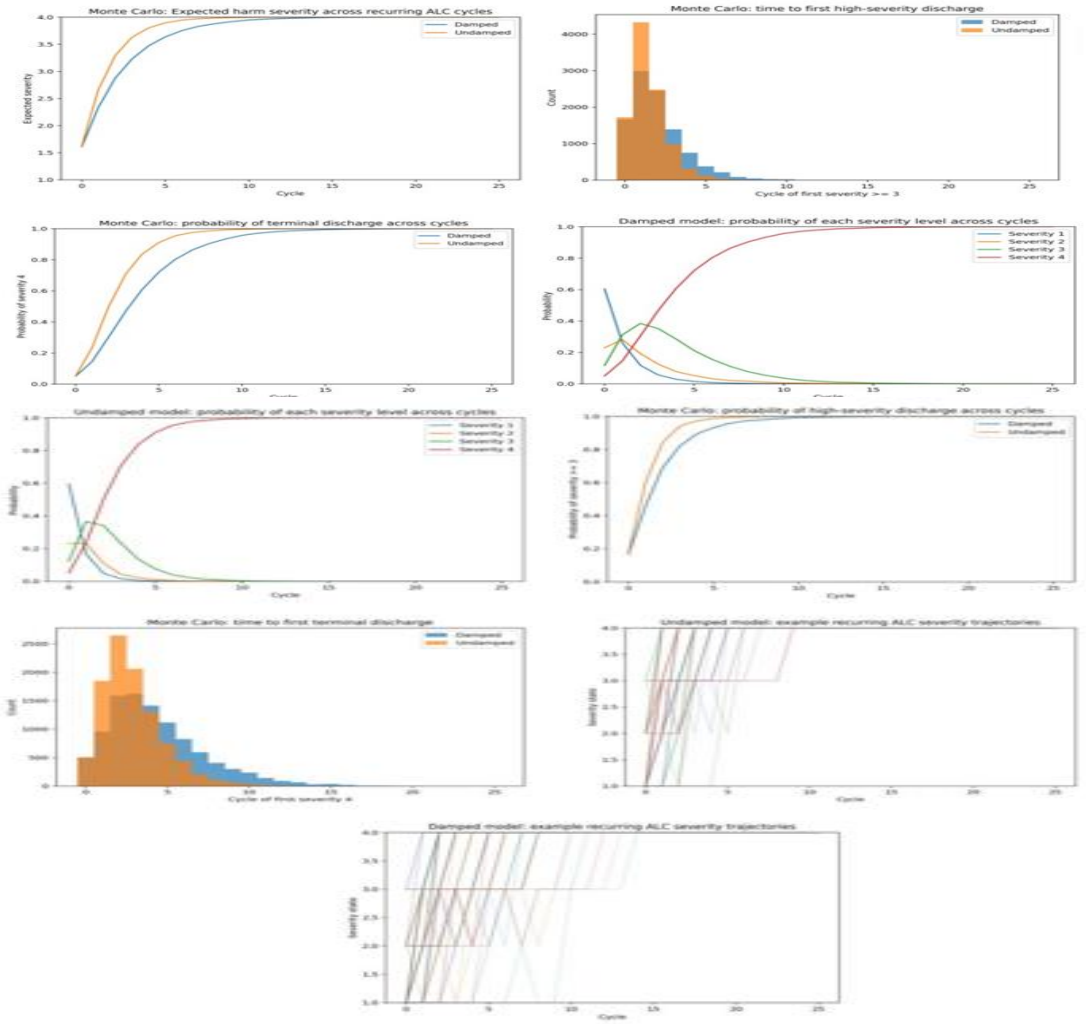

Figures 14a, 14b, 14c, 14d, 14e, 14f, 14g, 14h, 14i: Monte Carlo Simulation Results Over 10,000 Iterations Examining Harm Enactment Severity Under Differing Conditions

Importantly, harm discharge did not reset the system to baseline; instead, partial attenuation preserved residual intensity across cycles. This is reflected mathematically by the persistence of elevated transition probabilities even after downward transitions. Thus, escalation is governed not by single-event occurrence but by recursive gain accumulation, consistent with the theoretical distinction between Threshold 1 (probability of harm onset) and Threshold 2 (severity amplification under recursive instability). Overall, the Monte Carlo results support a nonlinear, gain-driven model of harm severity escalation in which the spectral radius of the recursive gain matrix provides a formal operational definition of Threshold 2.

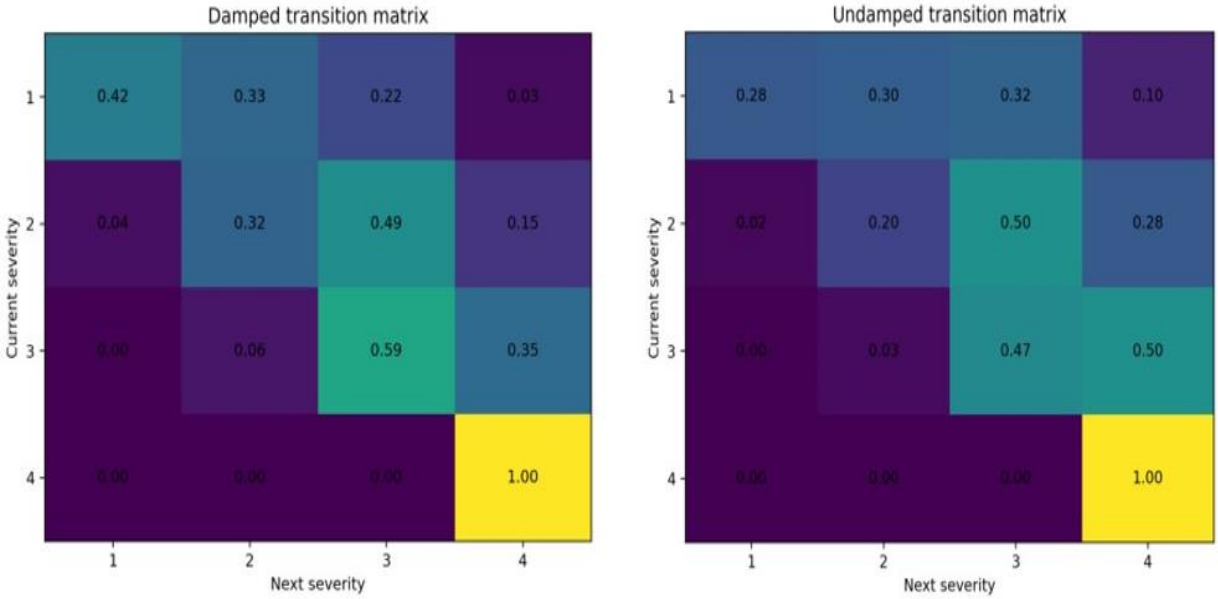

Figures 15a, 15b: Monte Carlo simulation 10,000 iterations showing transitions between severity levels expected by ALC intensity and recurrence for damped and counterfactual undamped samples

1.13. Harm Enactment Severity Section Conclusions

The present analysis demonstrates that harm enactment severity is not randomly distributed across recurrence states but instead clusters systematically within higher severity levels once the Anger Feedback Loop Cascade (ALC) becomes recursively active. Empirically, recurrence is disproportionately concentrated in Severity Level 3, with a marked discontinuity between low-severity corridor entry (Levels 1–2) and stabilized cycling under institutional visibility (Level 3). Terminal severity (Level 4) exhibits expected truncation effects due to lethality and legal incapacitation, limiting longitudinal observability but not negating its role as an asymptotic attractor. Across analytic layers, the results converge. Cross-sectional contingency analyses show a strong association between recurrence and higher severity classification. Discrete transition modeling indicates that recursive gain amplification shifts probability mass rightward across cycles.

Spectral radius interpretation formalizes Threshold 2 as the point at which recursive amplification exceeds damping, producing dynamic instability. Monte Carlo simulations illustrate progressive escalation under both dampened and undampened conditions, with the latter revealing a persistent trajectory toward terminal severity. Continuous time-domain approximation suggests that, even under treatment constraint, expected severity increases across annual cycles and likely underestimates escalation magnitude in unconstrained systems. Importantly, the model does not imply determinism. Harm enactment remains probabilistic and subject to intervention, attenuation, or reversal. However, when Epistemic Disorientation (EpD) and Affective Dysregulation (AD) are bilaterally amplifying and recursive gain exceeds damping, escalation becomes statistically probable and structurally self-reinforcing.

Under those conditions, harm severity progression reflects nonlinear system dynamics rather than isolated behavioral events. The findings therefore support a falsifiable and testable systems claim: recursive coupling among destabilized nodes predicts upward migration along a severity continuum, with observable cycling emerging at intervention-level harm and terminal severity representing a long-run attractor under insufficient damping. Further prospective validation and longitudinal calibration are necessary, but the present framework offers a unified probabilistic account of escalation, recurrence, and severity progression within high-risk human systems.

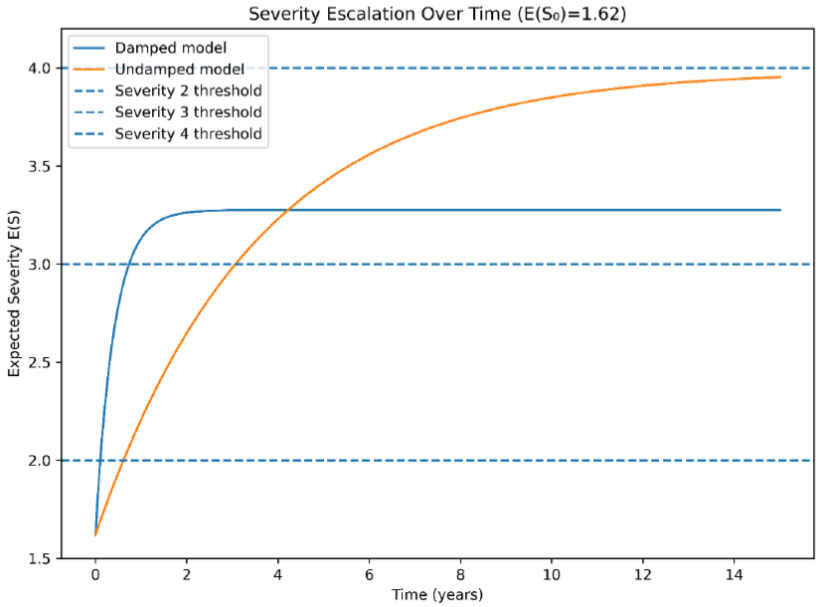

Figure 16: Severity Curves (Monte Carlo 10,000 Iterations) for Damped and Undamped Samples

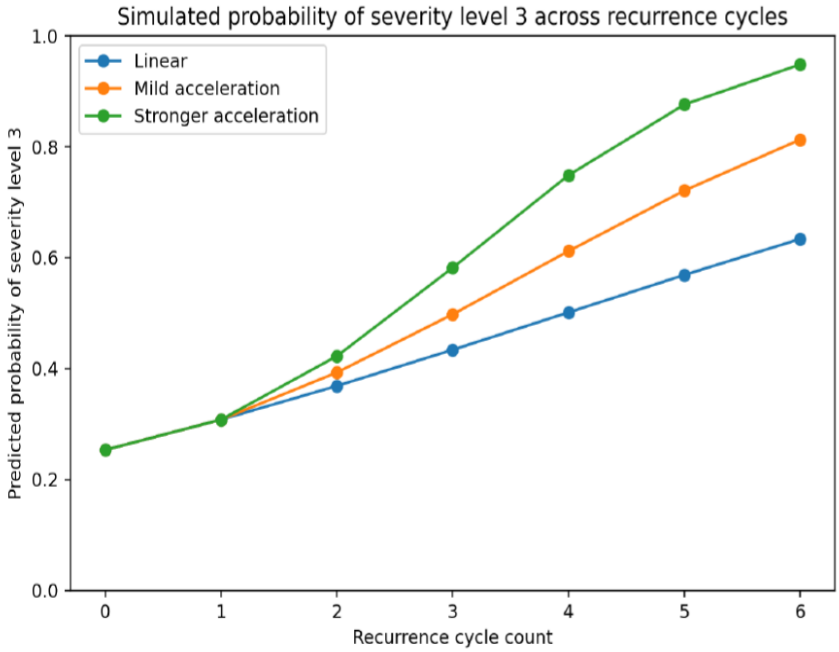

Figure 17: Empirical Probability of Recurrence Leading to Severity level 3 (Legal and Social Consequences for Harm Behavior)

• Interpretation

➢ Severity Levels 1–2 likely represent corridor entry but are under-sampled.

➢ Severity Level 3 marks stabilized cycling under institutional visibility.

➢ Severity Level 4 exhibits structural truncation bias.

➢ Recurrence strongly predicts upward movement along the severity continuum.

➢ Even under treatment damping, expected severity increases across cycles.

Given that all samples were drawn from populations under supervision or intervention, the observed ΔE(S) likely underestimates the undamped escalation magnitude. Using time-domain conversion with t_0 = 1.62as the onset expected severity, the fitted yearly recursive-gain rates from the trimmed recurrence intervals, the severity-time model is:

$$E(S_{max} - (S_{max} - 1.62)e^{-\gamma t}$$

with:
Damped: S_{max} = 3.275, γ = 2.433per year
Undamped: S_{max} = 3.986, γ = 0.285per year
From that, the estimated times to each remaining severity level are:

(i) Damped
• Reach Severity 2.0: 0.11 years (~39 days)
• Reach Severity 3.0: 0.74 years (~269 days)
• Reach Severity 4.0: not reached under the fitted damped asymptote
• (S_{max} = 3.275, so the curve saturates below 4)

(ii) Undamped
• Reach Severity 2.0: 0.61 years (~225 days)
• Reach Severity 3.0: 3.07 years (~1122 days)
• Reach Severity 4.0: not reached exactly because the fitted asymptote is 3.986, not 4.00

So, for the undamped case, the more honest way to express "near-Level-4" is:
• Reach 3.50: 5.56 years
• Reach 3.90: 11.63 years
• Reach 3.95: 14.68 years

(iii) Interpretation
With t_0 = 1.62:
• The damped model moves quickly into the Level-3 corridor and then plateaus.
• The undamped model escalates more gradually in calendar time, but it continues climbing toward terminal severity rather than stabilizing in the Level-3 range.
The current fitted structure implies:
•Detection-level severity (Level 3) emerges relatively early under damping,
• but terminal severity is a long-run undamped destination rather than an immediately reached state.

Estimated Time to Reach Harm Severity Levels Given $E(S_0)$= 1.62

Model Condition	Asymptotic Severity S_{max}	Gain γ (per year)	Time to Severity 2.0	Time to Severity 3.0	Time to Severity 4.0
Damped	3.275	2.433	0.11 years (39 days)	0.74 years (269 days)	Not reached
Undamped	3.986	0.285	0.61 years (225 days)	3.07 years (1,122 days)	Not reached exactly
Note. Estimates Derived from the Recursive Severity-Growth Function					

Table 11: Calendar Time for Severity Transition to Higher Level

$$E(S_t) = S_{max} - (S_{max} - 1.62)\, e^{-\gamma t}$$

with onset fixed at $E(S_0)$ = 1.62. In the damped model, the trajectory saturates below Severity 4 (S_{max} = 3.275), indicating stabilization in the Level-3 corridor rather than terminal escalation. In the undamped model, the trajectory approaches but does not mathematically equal Severity 4 because the fitted asymptote is S_{max} = 3.986. Thus, terminal severity is best interpreted as a long-run attractor rather than a finite exact crossing under the present fit. Under the damped model, expected severity rises rapidly into the Level-3 corridor and then plateaus, whereas under the undamped model, severity increases more gradually in calendar time but continues asymptotically toward terminal discharge.

2. Discussion and Implications

The present manuscript integrates three empirically distinct but dynamically related thresholds within a unified recursive systems framework of harm enactment. Threshold 1 identifies the probabilistic onset of overt harm enactment as recursive coupling between Epistemic Disorientation (EpD) and Affective Dysregulation (AD) intensifies. Threshold 2 identifies the subsequent escalation of Physiological Load (PL), Relational Revenge Orientation (RR) with Harm Enactment (HE) once recursive gain exceeds damping and the system enters sustained cycling. Harm Enactment (HE) is further defined by its severity. Harm Enactment severity is defined upon initiation and along a recurrent cyclical trend in escalating severity. The data support all three thresholds as operationally distinct phenomena.

2.1. Threshold 1: Probabilistic Entry into Overt Harm

Threshold 1 is defined in two stages.
• **Stage 1** reflects bilateral EpD × AD recruitment under increasing Cultural Narcissism (CN) and declining Worldview coherence (WV). Empirically, this stage corresponds to the parameter region in which the dominant eigenvalue (λ_1) approaches unity under base coupling conditions. Sensitivity analysis demonstrated that at a coupling scale of approximately 1.0, λ_1 crossed the stability boundary ($\lambda_1 \approx 1.00–1.05$), marking transition from dampened fluctuation to unstable amplification.
• **Stage 2** reflects the point at which recursive gain exceeds damping sufficiently to produce high probability of overt harm enactment. Monte Carlo simulations calibrated to the empirical transition structure showed that the probability of overt harm (P[overt HE] ≥ .50) clustered around Step 15–17 of recursive amplification under dampened conditions. The distribution of first breach timing was centered at approximately 16 steps (mean ≈ 16.3), indicating a relatively short escalation window once bilateral gain is established. The earliest enumerated calendar value was 29 days. Thus, Threshold 1 represents a statistically definable instability window in which overt harm becomes highly probable, not merely

possible.

2.2. Threshold 2: ALC Escalation with Recursive Gain Leads to Harm Enactment

After the recruitment of Physiological Load (PL) by EpD and AD, the recursive system seen in the WV CN EpD AD chain is further amplified by the introduction of Relational Revenge Orientation (RR). At this point, the ALC is fully activated and the whole subsystem is an ever-escalating multilateral, multidirectional, dynamic phase transitioning control parameter for the entire regime. The ALC is structurally self-excitatory and multi-node feedback gain ensures rapid exponential escalation. The system is essentially "pressurized" by ALC action. This pressure builds as the regime becomes more and more destabilized. Pressure release becomes a high probability and the method of discharge is Harm Enactment (HE).

Therefore, Threshold 2 is the calculable point at which ALC escalation makes overt HE probabilistically highly likely. From the onset of full node interaction, the scalar model of Threshold 2 repeatedly shows a dominant eigenvalue > 0. The introduction of two dampening effects, Exogenous Controls (EC) and Narcissistic Controls (CN), at varying levels, did not reduce dominant eigenvalue positive enumeration. Even at levels of 150% of empirical value, EC and CN did not reduce the probability of the HE discharges. At best, these restraining factors only delayed the time of discharge by 2-3 days. Monte Carlo simulations over 2,500 iterations confirmed the highly probabilistic nature of ALC discharge into HE. 99.5% of iterations had a probability of ALC discharge of >50%. The ALC escalation within these simulations produced a clustering of increasing probabilities of discharge at around 15 to 17 steps. The activation and escalation of the recursive self-excitatory ALC (all nodes in multi-directional feedback gains) set the conditions for entry into the harm enactment corridor with a highly probable overt harm enactment within days of initiation.

2.3. Harm Enactment Severity

Harm enactment severity addresses severity migration after initial harm entry. The first observed harm event across the dataset yielded an estimated expected severity of:

$$E(S)_{t0} = 1.62$$

This value places initial harm enactment between Severity Level 1 (sub-detection / intimidation / substance use escalation) and Level 2 (detectable harm without legal consequence), consistent with corridor entry rather than catastrophic onset. True recurrence analysis (excluding follow-up intervals > 5 years) yielded a mean inter-cycle interval of approximately 1.28 years (median ≈ 1.05 years), suggesting that a "cycle" in treated populations approximates one year of escalation–discharge–re-escalation. Importantly, all sampled cohorts were in treatment or institutional oversight, implying dampened dynamics. Across cycles, severity demonstrated nonlinear growth. Fitting the delta E(S) curve yielded an estimated multiplicative gain parameter of approximately:

$$g \approx 1.7$$

for the first three severity levels. This indicates that expected severity increases by roughly 70% of remaining headroom per cycle under dampened conditions. Ordered logistic and contingency analyses confirmed that recurrence probability is disproportionately concentrated at Severity Level 3 (legal/social consequence threshold), with χ^2 statistics increasing substantially when Level 4 (fatal/lethal) cases were included, reflecting rightward probability mass migration.

Projecting the fitted gain curve forward from:

$$E(S)_{t0} = 1.62$$

The expected severity approaches:

$$E(S) \approx 2.9$$

by approximately Cycle 21 under nonlinear acceleration. The probability of Severity Level 3 by that cycle exceeds 0.95 under modeled recursion. Terminal severity (Level 4) is empirically truncated in observational data due to lethality or legal incapacitation, but extrapolation of the fitted gain suggests that, absent damping, terminal severity becomes the asymptotic attractor within approximately 3–5 years (≈ 3–5 cycles in undampened systems; longer under treatment dampening).

2.4. Dampened vs. Undampened Dynamics

The observed dataset represents dampened systems—individuals already in treatment or under legal supervision. Despite this, recurrence remains highly prevalent and severity migration persists. Counterfactual simulations without damping show slower short-run escalation but greater long-run drift toward terminal severity due to uninterrupted recursive gain. The treated dataset exhibits more rapid early escalation because subjects enter observation at elevated severity, compressing visible cycles.

2.5. Implications for Intervention

The separation of thresholds carries practical implications:

- Threshold 1 identifies the window of maximal harm probability. Intervention at Stage or early Stage 2 may prevent corridor entry.
- Threshold 2 identifies the window when overt harm enactment becomes highly probable. Once ALC escalation begins, harm enactment becomes a high probability within days or weeks.
- Harm Enactment Severity identifies the severity of harm enactment from instantiation (severity 1.62 out of four) to five years (severity 3.96 without intervention, 2.95 with intervention).
- Cycle length (~1 year in treated populations) provides an approximate intervention horizon.
- Severity acceleration (~1.7 gain factor per cycle) quantifies the cost of delayed intervention.

Critically, the model does not imply determinism. Harm remains probabilistic and contingent on agency and intervention. However, when recursive gain exceeds damping ($\lambda_1 > 1$), the system enters a

statistically predictable escalation regime.

2.6. Theoretical Significance

The findings suggest that severe harm is not merely a product of extreme individuals but of extreme recursive system conditions. The convergence of spectral instability (Thresholds 1 and 2) and nonlinear severity gain (Harm Enactment Severity) supports a unified recursive model of harm enactment. If EpD and AD are not bilaterally amplifying, the model collapses. If recursive gain in the ALC does not predict Harm Enactment, Threshold 2 fails. If recurrence in harm enactment does not increase severity, Harm Enactment severity is false. Thus, the architecture is falsifiable.

In summary:

- Initial harm severity estimate: 1.62
- Estimated cycle length: ~1 year (treated sample)
- Gain in severity per cycle: ~1.7
- Cycles to near-terminal severity: ~20+ under dampening; Approx. 3-5 under undamped conditions
- Highest likelihood window of overt harm: recursive Steps 15–17 after instability onset or approximately 29 days.

These parameters collectively define a measurable escalation structure. Further prospective validation with true time-series node measurement is required. Nonetheless, the present findings provide a mathematically defined and empirically supported account of harm probability, recurrence, and severity progression within a destabilized system.

2.7. Statement of Generalizability

The present findings derive from large-scale aggregation of archival cohort, registry-based, case– control, and meta-analytic studies encompassing over 29 million cumulative participants across heterogeneous populations, geographic regions, and outcome domains. The dataset spans suicidality, substance use, interpersonal violence, chronic disease burden, relapse cohorts, and registry-confirmed mortality outcomes. Because construct coding was applied at the level of latent system variables (e.g., Epistemic Disorientation, Affective Dysregulation, Relational Revenge Orientation, Physiological Load) rather than diagnosis-specific categories, the model is not limited to any single psychiatric condition, demographic subgroup, or applied setting. Generalizability is therefore structural rather than diagnostic. The recursive coupling dynamics identified here reflect cross-domain convergence of effect sizes linking destabilized epistemic–affective states to behavioral and mortality outcomes. Heterogeneity estimates were moderate but stable, and leave-one-out and Monte Carlo perturbation procedures demonstrated persistence of threshold parameters and dominant eigenvalue positivity across sampling variation.

However, the present sample is disproportionately composed of treatment-engaged, court-supervised, or institutionally monitored cohorts. As such, escalation trajectories observed in this dataset likely represent dampened system expressions. The model therefore generalizes most directly to high-risk populations under observational or institutional constraint, and more cautiously to untreated general-population contexts. Prospective validation in longitudinal community samples is necessary to refine time calibration and population-specific risk magnitudes. Importantly, the model does not assume universality of escalation for all individuals. Rather, it specifies conditional generalizability: when recursive coupling among EpD, AD, RR, and PL exceeds damping constraints, escalation becomes probabilistically likely. The generalizability claim is thus mechanistic and contingent, not categorical.

2.8. AI Use Disclosure Statement

Artificial intelligence (AI) tools were used in a limited and assistive capacity during manuscript preparation. Specifically, a large language model was utilized to support language refinement, structural organization, and clarity of exposition. The AI tool was not used to generate original empirical data, conduct statistical analyses, derive mathematical results, determine parameter values, or make inferential decisions. All analytic procedures including data extraction, construct coding, effect-size transformation, meta-analytic pooling, Monte Carlo simulation, transition modeling, eigenvalue computation, and severity estimation were independently designed, executed, and verified by the author. All model specifications, statistical computations, dataset construction, and interpretive conclusions reflect the author's independent scholarly work. The author reviewed, edited, and takes full responsibility for the final content of the manuscript. AI assistance was confined to drafting support and did not replace scientific judgment, methodological decision-making, or data interpretation.

References

1. Park, C. L. (2010). Making sense of the meaning literature: an integrative review of meaning making and its effects on adjustment to stressful life events. *Psychological bulletin, 136*(2), 257.
2. Eriksson, M., & Lindström, B. (2005). Validity of Antonovsky's sense of coherence scale: a systematic review. *Journal of Epidemiology & Community Health, 59*(6), 460-466.
3. King, L. A., & Hicks, J. A. (2021). The science of meaning in life. *Annual review of psychology, 72*(1), 561-584.
4. Sisto, A., Vicinanza, F., Campanozzi, L. L., Ricci, G., Tartaglini, D., & Tambone, V. (2019). Towards a transversal definition of psychological resilience: a literature review. *Medicina, 55*(11), 745.
5. Winger, J. G., Adams, R. N., & Mosher, C. E. (2016). Relations of meaning in life and sense of coherence to distress in cancer patients: A meta-analysis. *Psycho-oncology, 25*(1), 2-10.
6. Flensborg-Madsen, T., Ventegodt, S., & Merrick, J. (2005). Sense of coherence and physical health. A review of previous findings. *The scientific world Journal, 5*(1), 665-673.
7. Parrott, D. J., Swartout, K. M., Eckhardt, C. I., & Subramani, O. S. (2017). Deconstructing the associations between executive functioning, problematic alcohol use and intimate partner aggression: A dyadic analysis. *Drug and alcohol review, 36*(1), 88-96.

8. Wong, I., & Denson, T. F. (2025). Understanding the mechanisms underlying the association between insecure attachment and intimate partner violence (IPV): Meta-analyses using two meta-analytical methods and a systematic review of mediators. *Clinical Psychology Review,* 102645.
9. Leo, D., Izadikhah, Z., Fein, E. C., & Forooshani, S. A. (2021). The effect of trauma on religious beliefs: A structured literature review and meta-analysis. Trauma, Violence, & *Abuse, 22*(1), 161-175.
10. Davidson, R. J., Putnam, K. M., & Larson, C. L. (2000). Dysfunction in the neural circuitry of emotion regulation--a possible prelude to violence. *Science, 289*(5479), 591-594.
11. McEwen, B. S. (2007). Physiology and neurobiology of stress and adaptation: central role of the brain. *Physiological reviews, 87*(3), 873-904.
12. McEwen, B. S. (2008). Central effects of stress hormones in health and disease: Understanding the protective and damaging effects of stress and stress mediators. *European journal of pharmacology, 583*(2-3), 174-185.
13. Klonsky, E. D., May, A. M., & Saffer, B. Y. (2016). Suicide, suicide attempts, and suicidal ideation. *Annual review of clinical psychology, 12*(1), 307-330.
14. Klonsky, E. D., Qiu, T., & Saffer, B. Y. (2017). Recent advances in differentiating suicide attempters from suicide ideators. *Current opinion in psychiatry, 30*(1), 15-20.
15. Klonsky, E. D., Pachkowski, M. C., Shahnaz, A., & May, A. M. (2021). The three-step theory of suicide: Description, evidence, and some useful points of clarification. *Preventive medicine, 152*, 106549.
16. Garland, E., Gaylord, S., & Park, J. (2009). The role of mindfulness in positive reappraisal. *Explore, 5*(1), 37-44.